

PERFORMANCE OF SOLAR HEATING SYSTEMS  
UTILIZING PHASE CHANGE ENERGY STORAGE

BY

DENNIS JOHN MORRISON  
MASTER OF SCIENCE  
(MECHANICAL ENGINEERING)  
UNIVERSITY OF WISCONSIN-MADISON

1976

#### ACKNOWLEDGEMENT

I am extremely grateful for the opportunity of working with my advisor, Dr. S. I. Abdel-Khalik, whose patient guidance made the completion of this thesis possible. I am indebted to Professors W. A. Beckman and J. A. Duffie of the University of Wisconsin for their supervision and support during my stay at the Solar Energy Laboratory. I would also like to thank my friends at the Solar Energy Laboratory for their invaluable assistance and numerous suggestions. Financial support by the Energy Research and Development Administration, through Contract No. E(11-1)-2588, is acknowledged.

PERFORMANCE OF SOLAR HEATING SYSTEMS  
UTILIZING PHASE CHANGE ENERGY STORAGE

By

Dennis John Morrison

A thesis submitted in partial fulfillment of  
the requirements for degree of

---

MASTER OF SCIENCE  
(Mechanical Engineering)

at the

University of Wisconsin-Madison

1976

## TABLE OF CONTENTS

		Page
	LIST OF TABLES . . . . .	.iii
	LIST OF FIGURES . . . . .	iv
	NOMENCLATURE . . . . .	.vii
	SUMMARY . . . . .	ix
CHAPTER 1	INTRODUCTION . . . . .	1
	1.1 Background . . . . .	1
	1.1.1 Material Selection, Testing and Containment . . . . .	3
	1.1.2 Theoretical Modeling . . . . .	6
	1.2 Objectives . . . . .	11
CHAPTER 2	PERFORMANCE OF AIR-BASED SYSTEMS UTILIZING PCES . . . . .	13
	2.1 Modeling PCES for Air-Based Systems . . . . .	13
	2.1.1 Negligible Fluid Capaci- tance Model for Air-Based Systems . . . . .	15
	2.1.2 Infinite NTU Model for Air- Based Systems . . . . .	19
	2.1.3 Variable Properties . . . . .	19
	2.1.4 Summary of Computing Capabilities . . . . .	20
	2.2 Method of Solution . . . . .	21
	2.2.1 Finite Differencing Scheme for NFC Model . . . . .	22
	2.2.2 Criteria for Stability and Accuracy . . . . .	25
	2.2.3 Incorporation into TRNSYS . . . . .	26
	2.3 Air-Based System Description and Control Strategy . . . . .	29
	2.4 Results for Air-Based Systems . . . . .	34

CHAPTER 3	PERFORMANCE OF LIQUID-BASED SYSTEMS UTILIZING PCES . . . . .	54
3.1	Modeling PCES for Liquid-Based Systems . . . . .	54
3.1.1	Infinite NTU Model for Liquid-Based Systems . . . . .	56
3.1.2	Variable Properties . . . . .	58
3.2	Method of Solution . . . . .	59
3.3	Liquid-Based System Description and Control Strategy . . . . .	59
3.4	Results for Liquid-Based Systems . . . . .	65
CHAPTER 4	DISCUSSION, CONCLUSIONS AND RECOMMEN- DATIONS . . . . .	76
4.1	Recommendations . . . . .	81
APPENDIX A	Weather Data . . . . .	83
APPENDIX B	Computer Listings . . . . .	84
APPENDIX C	Considerations When Using Finite Difference Approximations With an Infinite NTU Model . . . . .	98
BIBLIOGRAPHY	. . . . .	102

---

LIST OF TABLES

---

TABLE		Page
1	Temperature Ranges for PCES Applications. . .	4
2	Parameters Selected for Air-Based System Simulations. . . . .	32
3	Properties of PCM's Investigated . . . . .	37

LIST OF FIGURES

FIGURE		Page
1	Typical PCES Unit Design. . . . .	7
2	Schematic of PCES Unit. . . . .	9
3	Nodal Representation of PCES Unit . . . . .	.23
4	Results of Stability Study. . . . .	.27
5	Air-Based System I. . . . .	.30
6	Air-Based System II . . . . .	.31
7	Variation of Solar-Supplied Fraction of Load with NTU and Storage Mass for Air-Based Systems Utilizing PCES. . . . .	.36
8	Variation of Solar-Supplied Fraction of Load with Storage Mass and Collector Area for Air-Based Systems Utilizing PCES in Madison . . . . .	.39
9	Variation of Solar-Supplied Fraction of Load with Storage Mass and Collector Area for Air-Based Systems Utilizing PCES in Madison . . . . .	.40
10	Variation of Solar-Supplied Fraction of Load with Storage Mass and Collector Area for Air-Based Systems Utilizing Rock Bed Storage in Madison. . . . .	.43
11	Variation of Solar-Supplied Fraction of Load with Storage Mass for Air-Based Systems Utilizing Sensible and Latent Heat Storage Media in Madison. . . . .	.44
12	Variation of Solar-Supplied Fraction of Load with Storage Volume for Air-Based Systems Utilizing Sensible and Latent Heat Storage Media in Madison. . . . .	.45
13	Variation of Solar-Supplied Fraction of Load with Storage Mass for Air-Based Systems Utilizing Sensible and Latent Heat Storage Media in Albuquerque. . . . .	.47

LIST OF FIGURES  
(Continued)

FIGURE		Page
14	Variation of Solar-Supplied Fraction of Load with Storage Volume for Air-Based Systems Utilizing Sensible and Latent Heat Storage Media in Albuquerque . . . . .	.48
15	Variation of Collector Efficiency with Storage Mass for Air-Based Systems Utilizing Sensible and Latent Heat Storage Media. . . . .	.50
16	Variation of the Fraction of Heating Season PCM Spends in Liquid State with Collector Area . . . . .	.52
17	Effect of Collector "Quality" on Performance of Air-Based Systems Utilizing Sensible and Latent Heat Storage Media . . . . .	.53
18	Liquid-Based System I. . . . .	.60
19	Liquid-Based System II . . . . .	.61
20	Liquid-Based System III. . . . .	.62
21	Variation of Solar-Supplied Fraction of Load with Storage Mass and Collector Area for Liquid-Based Systems Utilizing PCES in Madison. . . . .	.66
22	Variation of Solar-Supplied Fraction of Load with Storage Mass and Collector Area for Liquid-Based Systems Utilizing PCES in Albuquerque. . . . .	.67
23	Variation of Solar-Supplied Fraction of Load with Storage Mass and Collector Area for Liquid-Based Systems Utilizing Water Tank Storage in Madison. . . . .	.70

LIST OF FIGURES  
(Continued)

FIGURE		Page
24	Variation of Solar-Supplied Fraction of Load with Storage Mass for Liquid-Based Systems Utilizing Sensible and Latent Heat Storage Media in Madison. . . .	.71
25	Variation of Solar-Supplied Fraction of Load with Storage Volume for Liquid-Based Systems Utilizing Sensible and Latent Heat Storage Media in Madison. . . .	.72
26	Variation of Solar-Supplied Fraction of Load with Storage Mass for Liquid-Based Systems Utilizing Sensible and Latent Heat Storage Media in Albuquerque . . . .	.74
27	Variation of Solar-Supplied Fraction of Load with Storage Volume for Liquid-Based Systems Utilizing Sensible and Latent Heat Storage Media in Albuquerque. . .	.75

## NOMENCLATURE

A	-	cross sectional area of PCM
A <sub>c</sub>	-	collector area
A <sub>f</sub>	-	cross sectional area of circulating fluid channel
c	-	average specific heat of PCM
c <sub>f</sub>	-	average specific heat of circulating fluid
c <sub>ℓ</sub>	-	specific heat of PCM in liquid phase
c <sub>s</sub>	-	specific heat of PCM in solid phase
$\mathcal{F}$	-	fraction of load supplied by solar source
K	-	average thermal conductivity of PCM
K <sub>f</sub>	-	average thermal conductivity of circulating fluid
K <sub>ℓ</sub>	-	thermal conductivity of PCM in liquid phase
K <sub>s</sub>	-	thermal conductivity of PCM in solid phase
ℓ	-	length of PCES unit
m	-	flow rate of circulating fluid
N	-	number of PCES subroutine internal time steps
P	-	perimeter of PCM in PCES unit
PCM	-	phase change material
PCES	-	phase change energy storage
NTU	-	number of transfer units, defined on page 21
S <sub>max</sub>	-	maximum ratio between time step and time constant of the PCM and circulating fluid nodes which occurs in governing equations, defined on page 32

NOMENCLATURE  
(Continued)

$S_s$	-	maximum allowable value of $S_{max}$ for solution to be both stable and accurate, defined on page 35
$t$	-	time
$T$	-	PCM temperature
$T_f$	-	circulating fluid temperature
$T_{fo}$	-	circulating fluid temperature leaving PCES unit
$T_{ref}$	-	reference temperature when PCM internal energy is zero
$u$	-	PCM specific internal energy
$\bar{u}$	-	PCM nondimensional specific internal energy, defined page 21
$U$	-	overall heat transfer coefficient between PCM and circulating fluid when $m > 0$
$U'$	-	overall heat transfer coefficient between PCM and circulating fluid when $m = 0$
$z$	-	position along storage unit in flow direction
$\rho$	-	PCM density
$\rho_f$	-	circulating fluid density
$\zeta$	-	nondimensional position along storage unit in flow direction, defined on page 32
$\theta$	-	nondimensional PCM temperature, defined on page 32
$\theta_f$	-	nondimensional circulating fluid temperature, defined on page 32
$\psi$	-	combined PCM and circulating fluid internal energy, defined on page 68
$\tau$	-	nondimensional time, defined on page 32
$\lambda$	-	PCM latent heat
$\eta_c$	-	collector efficiency
$\chi$	-	PCM liquid fraction

## SUMMARY

Although there has been considerable interest in phase change energy storage (PCES) over the past thirty years, no work has been done to determine its effect on the performance of complete solar energy systems. Therefore, the main objectives of this work have been:

1. To develop a practical model describing the long-term transient behavior of a PCES unit.
2. To determine the effect of storage/exchanger NTU, storage mass, material properties, and location on system performance.
3. To compare the performance of systems utilizing PCES with those utilizing conventional sensible heat storage.

Six models of PCES units were developed each representing different levels of approximation. These were incorporated into the transient simulation program TRNSYS[14]. Long-term simulations were used to determine the performance of air-based and liquid-based solar heating systems utilizing sodium sulfate decahydrate and paraffin wax in Madison (WI) and Albuquerque (NM). The performance of systems utilizing conventional water tank and rock bed storage were simulated for comparison.

It is shown that system performance is relatively insensitive to the storage/ exchanger NTU within the practical design range. Hence, the results of this investigation are based on simulations which employed infinite NTU models.

Storage capacities per unit collector area of 7-20 Kg/ m<sup>2</sup> and 7-25 kg/ m<sup>2</sup> are recommended for Na<sub>2</sub>SO<sub>4</sub>·10H<sub>2</sub>O and paraffin wax respectively. Determination of the optimum storage size will depend upon system economics and location.

Over the range of practical storage sizes, systems utilizing sensible heat storage are shown to yield a higher solar-supplied fraction of the load than those utilizing PCES. However, for air-based systems, both the phase change materials investigated required considerably smaller storage volumes than the rock bed in order to achieve the same system performance. For liquid-based systems, Na<sub>2</sub>SO<sub>4</sub>·10H<sub>2</sub>O will require smaller storage volumes than a water tank to achieve the same system performance but paraffin wax will require roughly the same storage volume.

## CHAPTER 1

### Introduction

#### 1.1 Background

Practical solar heating or cooling systems must be capable of thermal energy storage due to the intermittent nature of the energy source. Surplus solar heat collected during the day must be stored for use at night or on a cloudy day. This storage can be accomplished in several forms among which are sensible heat, latent heat, and chemical storage.

In sensible heat systems, energy is stored through a change in temperature of the storage medium. The storage unit is charged or discharged by simply raising or lowering the temperature of a water tank in liquid-based systems, or a pebble bed in air-based systems. This method has been employed almost exclusively in systems to date because the materials are universally available, inexpensive, and have essentially unlimited lifetimes.

Chemical storage is a relatively new concept where energy is stored in the form of heats of chemical reactions, e.g. the dissociation of  $\text{SO}_3$  into  $\text{SO}_2$  and  $\text{O}_2$  or the hydration of  $\text{MgO}$  to form  $\text{Mg(OH)}_2$ . Such reactions can achieve very high densities of energy storage. Energy densities

as high as 20,000 Btu/ft<sup>3</sup> can be achieved in practical chemical storage systems.

Latent heat systems utilize the heat associated with a change in the physical phase of the storage material. Solid-liquid transitions are the most practical due to the relatively small accompanying volume change. For most materials, the amount of energy required for a phase change is very large compared to that involved in a change of temperature. For example, melting one kilogram of paraffin wax (latent heat = 209 KJ/KG and specific heat = 2.89 KJ/KG°C) would require seventy-two times the energy needed to raise its temperature one degree Celcius. Therefore, phase change energy storage (PCES) appears superior to sensible heat storage for two reasons: 1) it requires considerably smaller storage volumes, and 2) the possibility exists for improving the thermal performance of the system (i.e. higher collector efficiency and fraction of load supplied by solar) due to the nearly constant storage temperature and hence, a constant collector inlet temperature.

On the other hand, PCES has two major drawbacks: 1) most phase change materials (PCM's) are currently more expensive than either water or rock, and 2) PCES devices must also incorporate a heat exchanger. The heat transfer medium and the storage material are not the same as in water tank storage, nor is the storage material always a solid as in

the pebble bed storage. Consequently, the PCM must be packaged in containers which have large heat transfer areas to facilitate adequate rates of charging and discharging.

There has been much interest in PCES over the last thirty years with most of the work falling into two categories:

1. Material selection, testing and containment.
2. Theoretical modeling of PCES subsystems.

In the following, a brief review of earlier work in these two areas will be given.

#### 1.1.1 Material Selection, Testing and Containment

There are thousands of compounds and mixtures from which potential phase change materials can be selected. Hence, several recent investigations [2,3,4] have established selection criteria for PCM's. The following is a composite list of these criteria:

1. Melting point in the proper temperature range (see Table 1)
2. Large heat of fusion
3. Congruent melting
4. No supercooling
5. Small volume change
6. Stability
7. Nonflammable

8. Nontoxic
9. Noncorrosive
10. Commercially available
11. Low cost

Application	°C	°F
Air conditioning	5-15	41-59
Solar Heating	45-55	113-131
Absorption Refrigeration	190-120	194-248

TABLE I. Temperature ranges for PCES applications.

Based on these criteria, the field of candidate materials has been considerably reduced and a number of the more promising candidates (possibly 10 to 20% according to Denton [5]) have been examined experimentally.

Lane et al. [3] assessed some 20,000 materials and presented a list of 205 potential candidates which was narrowed to 30 using laboratory evaluation techniques. Similar studies were reported by Hale et al. [4], who screened 500 potential materials, and by the National Center for Energy Management and Power at the University of Pennsylvania [2,6] where a survey of inorganic hydrates, organic compounds, and organic eutectics was conducted. Experi-

mental testing of cycling and latent heat measurements by Lorsch et al. [2,6] resulted in the selection of Sunoco's P116 paraffin wax (latent heat = 209 KJ/KG) as a promising material for solar heating applications.

Sodium sulfate decahydrate (commonly known as Glauber's salt,  $\text{Na}_2\text{SO}_4 \cdot 10\text{H}_2\text{O}$ ) is representative of another class of potential materials, viz. salt hydrates. It has long been considered a promising material because of its high latent heat and low cost. Unfortunately, its latent heat degrades upon repeated thaw/freezing cycling. The anhydrous sodium sulfate settles out during melting and fails to recombine with water when refrozen. Until recently, all attempts to prevent the settling process by using thickeners or encapsulation have failed. However, Chahroudi [7] reports that the use of wood fiber can extend the cycle life of Glauber's salt to 300 cycles. Telkes [8] reports that a thixotropic thickener can prevent separation completely and extend the cycle life to 1000 cycles without detectable degradation. These claims, however, are based on experiments where the material is heated and cooled in a steady cyclic fashion with relatively short cycle times. It is not known how the material will respond in an actual system where the thaw/freezing cycles are irregular and extend over periods of hours.

A number of material encapsulation and containment techniques have been studied [2,3,6,8]. Storage/exchanger devices in a variety of sizes and configurations have been recommended [2,6]. Of all systems recommended to date, the least expensive uses plastic trays for containment of the PCM, mild steel module walls, and a conventional mild steel fuel tank [6]. A schematic diagram of a typical PCES heat exchanger is shown in Figure 1.

#### 1.1.2 Theoretical Modeling

Many theoretical models and computer programs for analyzing PCES systems have been reported in the literature [9-13]. Bannister [9], Schlosinger [10], Abbott [11], and Fixler [12] used finite difference computer methods to predict the temperature distribution and location of the melt front as a function of time. Leatherman [13] used analog computer simulation to analyze PCM components.

This investigation is based on unpublished work by Abdel-Khalik who developed a simple model for PCES units. The following assumptions were made:

1. Neglect differences between the physical properties of the liquid and solid phases of the PCM.
2. Neglect axial conduction in the circulating fluid.

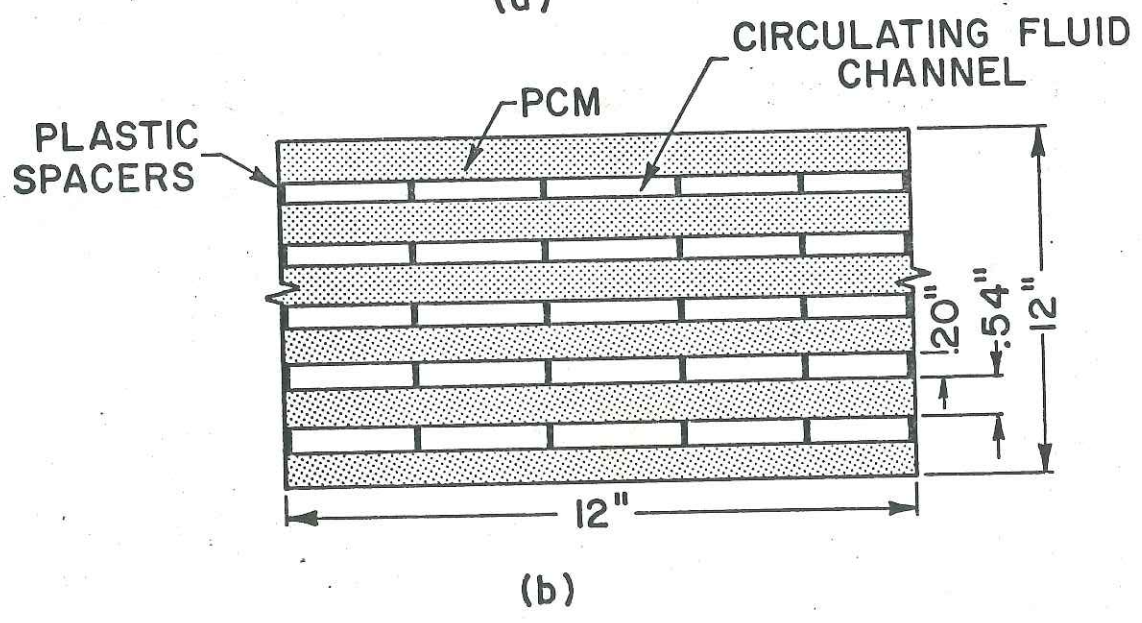
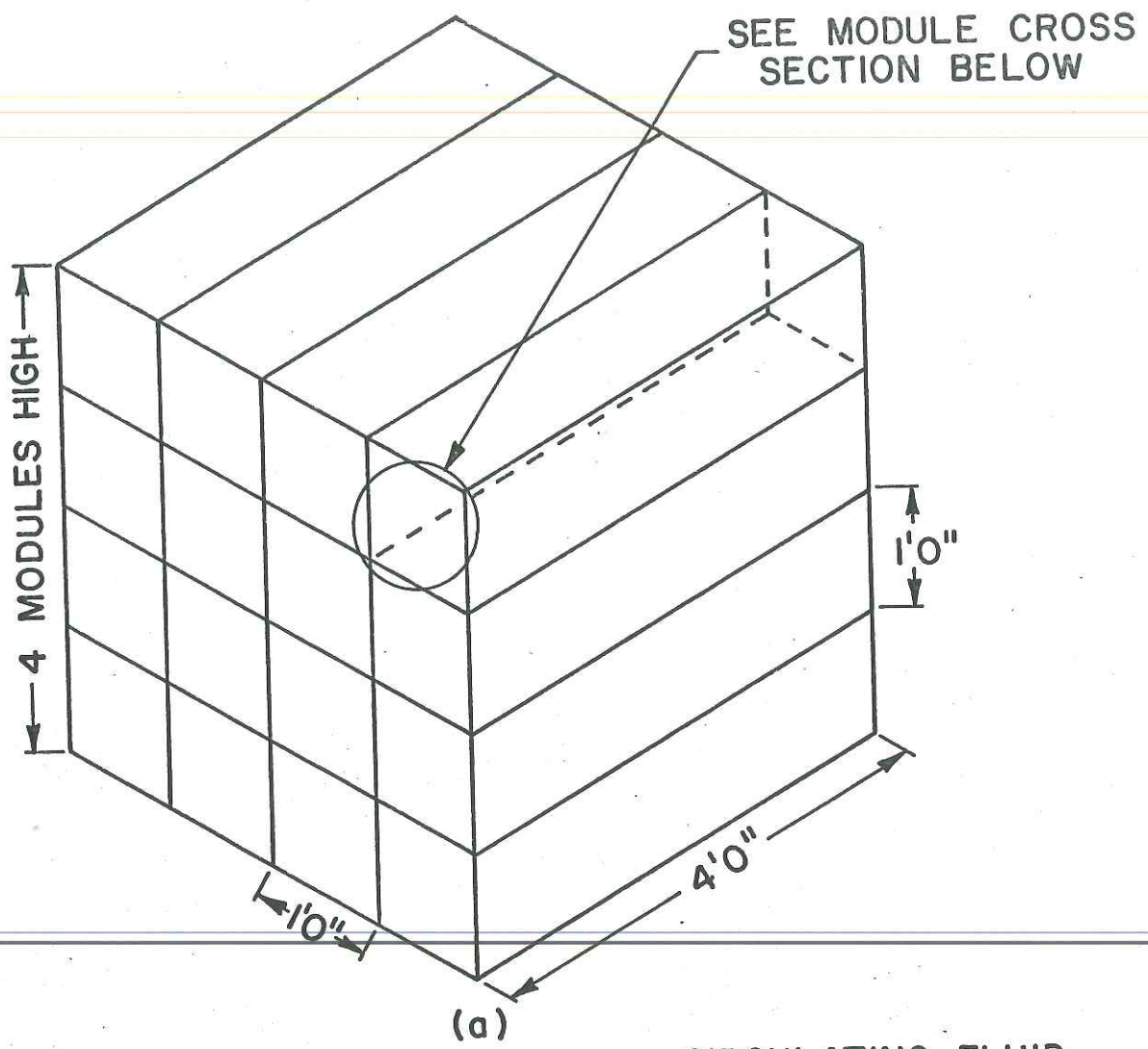


FIGURE 1. Typical PCES Unit Design.

3. The Biot number is sufficiently low such that temperature variations normal to the flow direction can be ignored.
4. Neglect heat losses to the surroundings.

Figure 2 shows the simplified PCES configuration considered. The PCM is placed in thin flat containers, or small tubes, of length  $l$ , total cross sectional area  $A$ , and wetted perimeter  $P$ . The heat transfer fluid passes through the storage unit at a constant rate  $\dot{m}$  with inlet temperature  $T_{fi}$ .

An energy balance for the PCM yielded the following differential equation:

$$\frac{\partial u}{\partial t} = \frac{k}{\rho} \frac{\partial^2 T}{\partial z^2} + \frac{UP}{\rho A} (T_f - T) \quad (1.1)$$

Here,  $u$ ,  $t$ ,  $k$ , and  $\rho$  are the specific internal energy, temperature, thermal conductivity and density of the phase change material,  $T_f$  and  $U$  are the circulating fluid temperature and overall heat transfer coefficient,  $t$  is time, and  $z$  is the flow direction.

The specific internal energy  $u$  is related to the temperature  $T$  and liquid fraction  $\chi$  by the relation:

$$u = c (T - T_{ref}) + \chi \lambda \quad (1.2)$$

for $T < T^*$	$\chi = 0$
for $T = T^*$	$0 \leq \chi \leq 1$
for $T > T^*$	$\chi = 1$

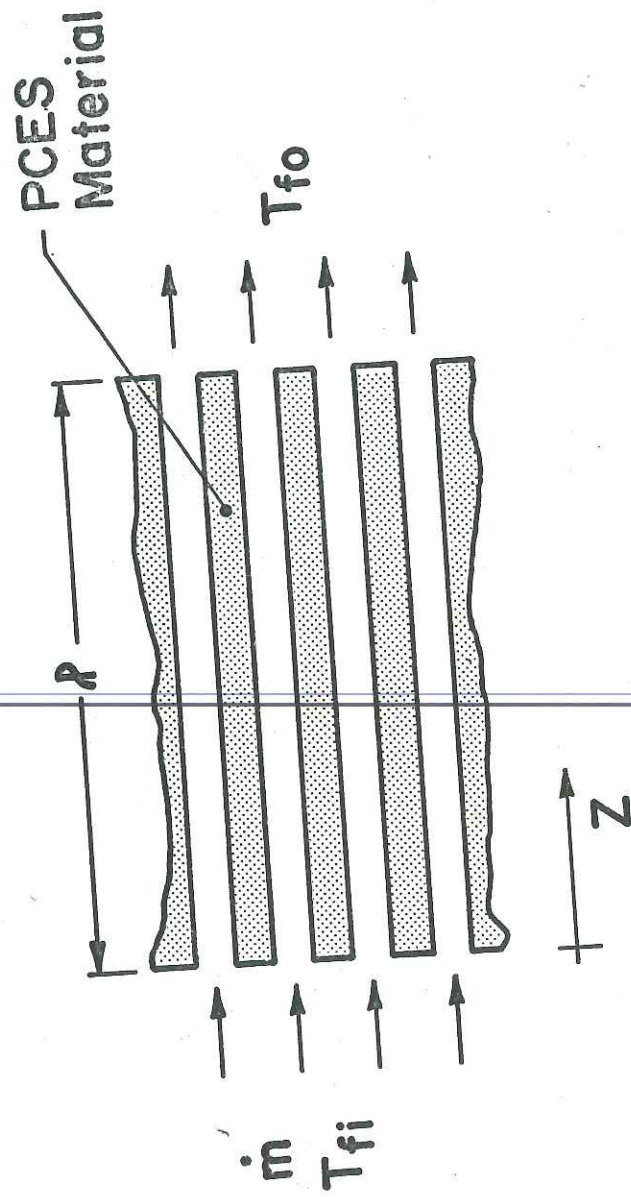


FIGURE 2. Schematic of PCES Unit.

Here,  $T^*$  is the melting temperature,  $\lambda$  is the latent heat,  $c$  is the specific heat, the  $T_{ref}$  is an arbitrary reference temperature when  $u$  is equal to zero.

The fourth assumption listed above leads to the following boundary conditions (i.e. no end losses):

$$\begin{aligned} \frac{\partial T}{\partial z} \Big|_{z=0} &= 0 \\ \frac{\partial T}{\partial z} \Big|_{z=l} &= 0 \end{aligned} \quad (1.3)$$

An energy balance for the circulating fluid yielded the following differential equation:

$$\frac{\partial T_f}{\partial t} + \frac{\dot{m}}{\rho_f A_f} \frac{\partial T_f}{\partial z} = \frac{UP}{\rho_f A_f c_f} (T - T_f) \quad (1.4)$$

Here,  $\rho_f$ ,  $A_f$ , and  $c_f$  are the density, flow area, and specific heat of the circulating fluid.

The inlet fluid temperature is an arbitrary function of time so that:

$$T_f(0, t) = f(t) \quad (1.5)$$

The derivatives in equations (1.1) and (1.4) were approximated using finite difference techniques and a computer program was written to determine the transient temperature history in the PCM for a given inlet fluid temperature variation,  $f(t)$ . The effects of system parameters on the sustained response of the PCES unit to a periodic square wave

inlet fluid temperature were investigated. The results showed that the circulating fluid capacitance, fluid residence time, and the overall heat transfer coefficient had a significant effect on system temperature response whereas the thermal conductivity did not. Necessary criteria for stability and accuracy were also developed; these will be discussed later.

## 1.2 Objectives

Prior to this investigation, no work had been done on simulating the performance of a complete solar energy system utilizing PCES. Therefore, the main objectives of this work have been:

1. To develop a practical model describing ~~the long-term transient behavior of a~~ PCES unit. This model is to be incorporated into TRNSYS [14].
2. To perform long-term simulations in order to determine the effects of shortage/exchanger NTU, storage mass, material properties, and location on system performance.
3. To compare the performance of systems utilizing PCES and those utilizing conventional water tank or pebble bed storage.

The remainder of this thesis is arranged as follows: Chapter 2 contains a description of the theoretical modeling, method of solution, system configuration and performance results for air-based solar heating systems. Chapter 3

contains this same information for liquid-based systems. Conclusions, discussion and recommendations are given in Chapter 4.

## CHAPTER 2

## PERFORMANCE OF AIR-BASED SYSTEMS UTILIZING PCES

Section 1 of this chapter describes the four models developed in this investigation for use in the simulation of air-based systems. Each one represents a different level of approximation. Section 2 describes the finite differencing scheme, stability and accuracy criteria, and incorporation of the PCES models into the transient simulation program TRNSYS [15]. Section 3 contains the configurations and control strategies for the systems simulated. The results for air-based systems are given in section 4.

## 2.1 Modeling PCES for Air-Based Systems

When incorporated into a solar heating system, a PCES unit has three modes of operation: charging, discharging and isolation. During charging and discharging the circulating fluid moves through the storage unit at constant rate  $\dot{m}$  (generally in opposite directions). These modes (referred to as "flow modes") can be described by the governing equations and boundary conditions given previously in section 1.1.2 (Equations 1.1 - 1.5). The storage unit is isolated when it is bypassed or when the heating system is off. Here the circulating fluid flow rate is zero and axial conduction will tend to even out the temperature distribution within the

the storage unit. For this mode (referred to as the "conduction mode"), the governing equations and boundary conditions for the PCM are exactly the same as for the flow modes. However, an energy balance for the circulating fluid now yields the following differential equation:

$$\frac{\partial T_f}{\partial t} = \frac{K_f}{C_f \rho_f} \frac{\partial^2 T_f}{\partial z^2} + \frac{U'P}{C_f \rho_f A_f} (T - T_f) \quad (2.1)$$

Here,  $K_f$  is the circulating fluid thermal conductivity and  $U'$  is the overall heat transfer coefficient when the fluid flow rate is zero.

The boundary conditions for the circulating fluid are as follows:

$$\left. \frac{\partial T_f}{\partial z} \right|_{z=0} = 0$$

$$\left. \frac{\partial T_f}{\partial z} \right|_{z=l} = 0 \quad (2.2)$$

The first computer model developed in this investigation was based upon the governing equations and boundary conditions given above for the three operating modes, viz. equations 1.1 - 1.5 for the flow modes and 1.1 - 1.3, 2.1 and 2.2 for the conduction mode. This model is general inasmuch as it can be used for either air-based or liquid-based systems. No restrictions are placed upon the type of circulating fluid since its capacitance is accounted for in the energy equations. However, computing costs were prohibitively high when air

was used as the circulating fluid. The capacitance of air is negligible when compared to that of any PCM. Hence, criteria for stability and accuracy require an extremely small time step. The development of an acceptable model for air-based systems required that the capacitance of the air be neglected.

The initial model described earlier is suitable for liquid-based systems where the capacitance of the circulating fluid is not negligible. It will be treated further in Chapter 3.

It should be emphasized that the models presented here assume that the PCM will behave ideally, i.e. the material properties will not degrade as a result of the cyclic operation of the system.

### 2.1.1 Negligible Fluid Capacitance Model for Air-Based Systems

As indicated above, for air-based systems the capacitance of the circulating fluid (air) is considerably less than that of the PCM. The following will show how the general model can be modified for these conditions.

The assumptions involved here are:

1. Neglect differences between the physical properties of the liquid and solid phases of the PCM.
2. Neglect axial conduction in the PCM and the circulating fluid in both modes.

3. The Biot number is sufficiently low such that temperature variations normal to the flow direction can be ignored.
4. Neglect all heat losses to the surroundings.
5. Neglect the capacitance of the circulating fluid.

Assumptions two and five are different from those in the original Abdel-Khalik model. Using that model, the thermal conductivity of the PCM was found to have no significant effect on the thermal response of the PCES unit. Therefore, axial conduction in the PCM was ignored in the flow mode for the negligible fluid capacitance (NFC) model.

The Flow Mode: Energy balances for the PCM and the air yield the following governing equations:

$$\frac{\partial u}{\partial t} = \frac{UP}{\rho A} (T_f - T) \quad (2.3)$$

and

$$\frac{\partial T_f}{\partial z} = \frac{UP}{\dot{m}c_f} (T - T_f) \quad (2.4)$$

The Conduction Mode: When the air flow rate through the storage unit is stopped, the governing equations become:

$$\frac{\partial u}{\partial t} = \frac{k}{\rho} \frac{\partial^2 T}{\partial z^2} \quad (2.5)$$

and

$$T_f = T \quad (2.6)$$

The boundary conditions and the subsidiary internal energy equations 1.2 remain unchanged.

The computer programming and subsequent analysis were simplified by the normalization of the governing equations and boundary conditions. The following variables and non-dimensional groups were defined:

$$\theta = (T - T_{ref}) / (T^* - T_{ref})$$

$$\theta_f = (T_f - T_{ref}) / (T^* - T_{ref})$$

$$\bar{u} = u / c (T^* - T_{ref})$$

$$\tau = t U P \ell / \rho v c$$

$$\zeta = z / \ell$$

$$NTU = U \rho \ell / \dot{m} c_f$$

$$K_1 = (KA / \ell) / U P \ell$$

$$K_2 = \lambda / c (T^* - T_{ref})$$

Substitution of these non-dimensional quantities into equations 2.3, 2.4, 2.5 and 2.6 yield the following equations:

The Flow Mode:

$$\frac{\partial \bar{u}}{\partial \tau} = (\theta_f - \theta) \quad (2.7)$$

$$\frac{\partial \theta_f}{\partial \zeta} = NTU (\theta - \theta_f) \quad (2.8)$$

The Conduction Mode:

$$\frac{\partial \bar{u}}{\partial \tau} = K_1 \frac{\partial^2 \theta}{\partial \zeta^2} \quad (2.9)$$

$$\theta_f = \theta \quad (2.10)$$

The boundary conditions for the PCM for both modes are now:

$$\begin{aligned} \left. \frac{\partial \theta}{\partial \zeta} \right|_{0, \tau} &= 0 \\ \left. \frac{\partial \theta}{\partial \zeta} \right|_{1, \tau} &= 0 \end{aligned} \quad (2.11)$$

For the circulating fluid in the flow mode, the boundary condition becomes:

$$\theta_f(0, \tau) = F(\tau) \quad (2.12)$$

In the conduction mode, the boundary conditions for the circulating fluid are:

$$\begin{aligned} \left. \frac{\partial \theta_f}{\partial \zeta} \right|_{0, \tau} &= 0 \\ \left. \frac{\partial \theta_f}{\partial \zeta} \right|_{1, \tau} &= 0 \end{aligned} \quad (2.13)$$

The subsidiary equations (1.2) relating  $\bar{u}$ ,  $\theta$ , and  $\bar{\chi}$  are now:

$$\begin{aligned} \bar{u} &= \theta + K_2 \bar{\chi} \\ \text{for } \theta < 1 & \quad \bar{\chi} = 0 \\ \text{for } \theta = 1 & \quad 0 \leq \bar{\chi} \leq 1 \\ \text{for } \theta > 1 & \quad \bar{\chi} = 1 \end{aligned} \quad (2.14)$$

### 2.1.2 Infinite NTU Model for Air-Based Systems

The modeling of PCES can be further simplified and computational costs considerably reduced if it is assumed that the storage unit has an NTU of infinity. Hughes et al. [14] examined the effect of NTU on the overall performance of a heating system utilizing rock bed storage. They concluded that for all practical purposes an infinite NTU model can adequately describe the rock bed. The extension of this hypothesis to PCES systems was investigated in this work.

The governing equations for the conduction mode, the subsidiary internal energy equations, and all boundary conditions remain the same as for the NFC model. However, the flow mode equations for the PCM and air become:

$$\frac{\partial u}{\partial t} = -\frac{\dot{m}c_f}{\rho A} \frac{\partial T}{\partial z} \quad (2.15)$$

and

$$T_f = T \quad (2.16)$$

### 2.1.3 Variable Properties

The thermal conductivity and specific heat of PCM's may vary significantly between the solid and liquid phases. For example, the specific heat of solid sodium sulfate decahydrate is 1.95 KJ/KG°C compared to 3.26 KJ/KG °C for the liquid.

To account for this variation, the subsidiary equation 1.2 relating  $u$ ,  $t$  and  $\chi$  can be modified as follows:

$$\begin{aligned}
 u &= c_s (T-T_{ref}) && \text{for } T < T^* \\
 u &= c_s (T-T_{ref}) + \chi\lambda && \text{for } T = T^* \\
 u &= c_s (T-T_{ref}) + \lambda + c_l(T-T^*) && \text{for } T > T^*
 \end{aligned}
 \tag{2.17}$$

Here,  $c_s$  and  $c_l$  are the specific heat of the solid and liquid phases respectively.

The local value of the thermal conductivity can be estimated by:

$$K = \chi K_l + (1-\chi)K_s \tag{2.18}$$

$K_l$  and  $K_s$  are the thermal conductivity of the solid and liquid phases.

#### 2.1.4 Summary of Computing Capabilities

Four models have been developed for use in the simulation of air-based systems utilizing PCES. The first was a generalized model based on work done by Abdel-Khalik. The second neglected the capacitance of the air in order to lower the computing costs to an acceptable level. An infinite NTU model further lowered computing costs and allowed the investigation of storage/exchanger heat transfer parameters to be taken to a logical limit. Finally, the restriction of

equal solid and liquid properties was removed to enable the accurate simulation of materials exhibiting significant property variations.

Again, it is important to stress the fact that the above models assume that the PCM will behave in an idealized way. In other words, such phenomena as property degradation, supercooling, and crystallization are not accounted for. These phenomena may significantly affect the system performance. However, this does not diminish the importance of the results that follow since they represent an upper bound to the performance of a system utilizing PCES. This knowledge will be invaluable in comparing different storage media and outlining areas for future research.

## 2.2 Method of Solution

Finite differencing techniques were used to solve the governing equations for all above models. Separate computer programs were written for the different levels of approximation indicated earlier, viz. the finite NTU NFC model, the infinite NTU case, and the variable properties model. These programs were written in the form of subroutines compatible with the requirements of TRNSYS [15]. They were then used to simulate the performance of a typical solar heating system.

In order to illustrate the numerical techniques used, the finite differencing scheme for the flow mode of the finite NTU NFC model is outlined below.

### 2.2.1 Finite Differencing Scheme for the NFC Model

The storage unit is divided into N axial nodes as shown in Figure 3. At the beginning of each time step, the PCM internal energy and air temperature for the different axial nodes, along with the current inlet fluid temperature are known.

Forward differencing techniques are then used to update these values. For example, equations 2.7 and 2.8 can be written as follows:

$$\frac{\bar{u}_i^{v+1} - \bar{u}_i^v}{\Delta\tau} = (\theta_{fi}^v - \theta_i^v) \quad i = 1, 2, \dots, N \quad (2.19)$$

and

$$\frac{\theta_{fi+1}^{v+1} - \theta_{fi}^{v+1}}{\Delta\zeta} = \text{NTU} (\theta_i^v - \theta_{fi}^v) \quad i = 2, 3, \dots, N \quad (2.20)$$

Here,  $i$  represents the nodal position shown in Figure 3,  $v$  and  $v+1$  signify values at the old and new time step,  $\Delta\tau$  is the non-dimensional time step, and  $\Delta\zeta$  is the non-dimensional nodal spacing.

Equations 2.19 and 2.20 can be rearranged as follows:

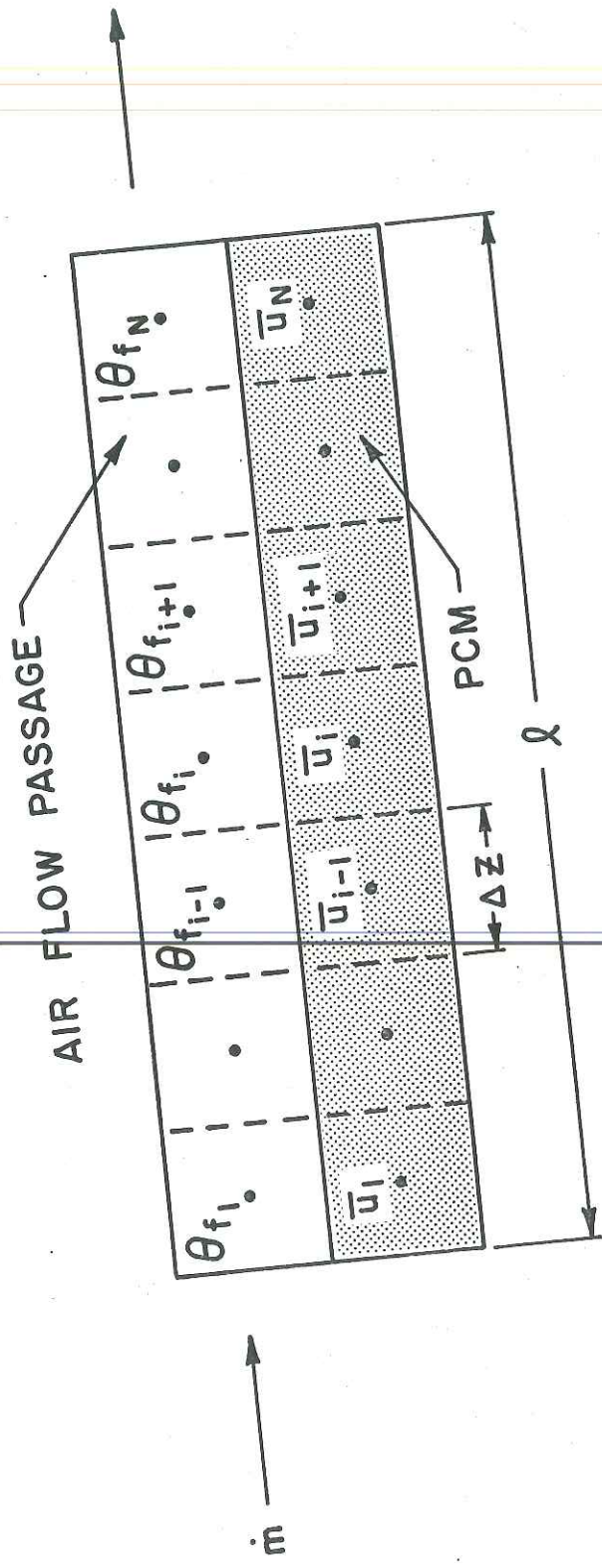


FIGURE 3. Nodal Representation of PCES Unit.

$$\bar{u}_i^{v+1} = \bar{u}_i^v + \Delta\tau (\theta_{fi}^v - \theta_i^v) \quad i = 1, 2, \dots, N \quad (2.21)$$

and

$$\theta_{fi+1}^{v+1} = \theta_{fi}^{v+1} + \Delta\zeta \text{ NTU } (\theta_i^v - \theta_{fi}^v) \quad i = 2, 3, \dots, N \quad (2.22)$$

The above equations can also be obtained by making energy balances for the different axial nodes over the time interval  $v\Delta\tau$  to  $(v+1)\Delta\tau$ . Equation 2.21 simply indicates that the internal energy gained by the PCM over the time step is equal to the heat transferred from the air to the PCM during that interval. Similarly, equation 2.22 states that the change in the air enthalpy as it passes over a given node is equal to the amount of heat added by convection.

Knowing the values of  $u_i^v$ ,  $\theta_i^{v+1}$ ,  $\theta_{fi}^v$ ,  $i = 1, 2, \dots, N$ , and the new inlet fluid temperature  $\theta_{fi}^{v+1}$ , equations 2.21 and 2.22 are used to determine the internal energies and fluid temperatures at the end of the time step.

The new fluid temperatures are calculated first, followed by the internal energy of each corresponding PCM node. The temperature and quality at each PCM node can then be updated using the subsidiary equation 2.14. The same equations are used when the flow direction is reversed by simply renumbering the axial nodes. Similar procedures are used for finite differencing the conduction mode equations. The mode of operation is determined internally by checking the magnitude and direction of the air flow.

### 2.2.2 Criteria for Stability and Accuracy

The stability and accuracy of the numerical solution will depend upon the magnitude of the time step used while the spatial resolution will obviously depend upon the number of axial nodes. In equation 2.21,  $\Delta\tau$  is the ratio between the time step  $\Delta t$  and the time constant of the "lumped" PCM node  $[\rho(v/\ell)\Delta zc/UP\Delta z]$ . In equation 2.22  $\Delta\zeta_{NTU}$  is the number of transfer units for each axial node. In order for the numerical solution to be stable, the ratio between the time step and the time constant of each node should be less than or equal to 0.5. When axial conduction is taken into account, the Fourier modulus of each node should also be less than or equal to 0.5. Similar restrictions are imposed on the fluid nodes if their capacitance is taken into account.

It should be emphasized that accuracy considerations may necessitate a smaller time step than that imposed by the above stability criteria. A sensitivity study was performed using the original Abdel-Khalik model to determine the effect of the number of nodes and time step on the accuracy of the solution. The system was subjected to a square wave inlet fluid temperature (see inset in Figure 4). The system parameters were selected such that the ratios between the time step  $\Delta t$  and the time constants of the PCM nodes and the fluid nodes were equal. This ratio, hereafter labeled  $S_{max}$ , was varied between 0.025 and its maximum allowable value of 0.50.

Typical results are shown in Figure 4 where the non-dimensional temperature of the first PCM node,  $\theta(1,\tau)$  (defined on page 17) is plotted against the non-dimensional time  $\tau$  for different values of the non-dimensional time step  $S_{max}$ .

As the time step decreases, the PCM temperature response approaches a unique distribution. Accuracy within five percent is achieved for  $S_{max}$  less than or equal to 0.1.

Another sensitivity study was performed after incorporating the PCES models into the transient simulation program, TRNSYS (see section 2.2.3). It was shown that a value of  $S_{max}$  as large as 0.4 could be used without significantly affecting the performance results of a complete solar heating system.

### 2.2.3 Incorporation into TRNSYS

TRNSYS is a transient simulation program developed at the University of Wisconsin Solar Energy Laboratory for the simulation of solar energy systems. It is a collection of subroutines which model the individual components present in a solar energy system such as the collectors, pumps, valves, storage tank and load. The ducts, pipes and wires which connect the components of a real system are represented by the flow of information between subroutines. The user need only supply TRNSYS with the system configuration, component

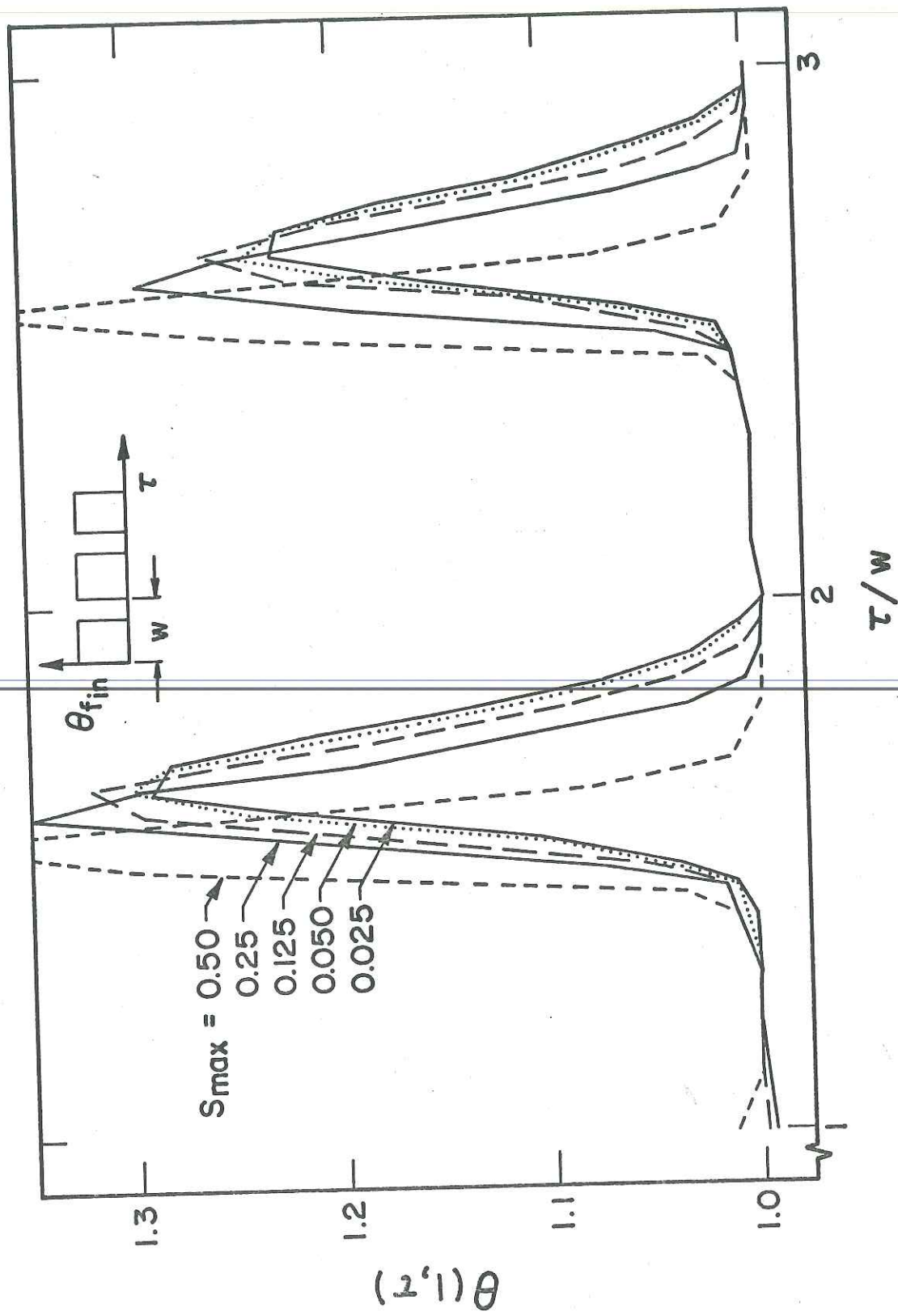


FIGURE 4. Results of Stability and Accuracy Study.

parameters and weather data. A complete description of the program is available in the TRNSYS Manual [15].

The incorporation of the PCES models into TRNSYS subroutines produced one major obstacle. The time step required for the PCES models to be stable was too restrictive for economic utilization of TRNSYS. Depending upon the number of nodes, the size of the storage unit, and storage material properties, the time step required by the PCES subroutines was 3 to 50 times smaller than that required by the other TRNSYS subroutines.

This problem was solved by running TRNSYS at an optimum time step (usually 15 minutes) and subdividing it within the PCES subroutine in order to meet the storage unit stability criteria (i.e. a time step within a time step). At the beginning of the simulation, the PCES subroutine calculates the maximum non-dimensional time step  $S_{max}$  corresponding to  $\Delta t$  used in other TRNSYS components and compares it to the value selected for stability and accuracy  $S_s$ . If necessary, the TRNSYS time step  $\Delta t$  is divided by an integer  $N$  to yield the storage unit time step  $\Delta t'$  where  $N$  is defined as follows.

$$N = \frac{S_{max}}{S_s} + 1 \quad (2.23)$$

The factor of 1 in equation 2.23 allows for the truncation which will occur when the quotient of  $S_{max}$  and  $S_s$  is converted to an integer.

For every TRNSYS time step, the PCES subroutine equations are solved  $N$  times using a time step of  $\Delta t'$ .

The number of nodes is a subroutine variable specified

by the user (usually 5 to 10). However, for the finite NTU model the number of nodes is selected such that  $NTU \Delta\zeta$  is less than or equal to 0.5. When this criteria is not met, the user supplied nodal spacing is modified internally. For the infinite NTU model, the finite difference approximation will tend to smoothen out the temperature front propagating through the storage unit. In this case, the number of nodes can significantly effect the system performance (Appendix C).

The procedure described above for selecting the time step guarantees the lowest possible computing costs and removes the responsibility of checking for stability and accuracy considerations from any future user.

### 2.3 Air-Based System Description and Control Strategy

The two air-based systems simulated in this investigation are shown in Figures 5 and 6. System I is a standard air-based system which can utilize either rock bed storage or PCES. The system configuration and control strategy are identical for both storage media. System II is the same as System I except that it has no storage capability. The parameters selected for the system components are shown in Table 2.

System I has three operational modes. The first occurs when solar energy is available for collection and the space heating load is not zero. Here, air is circulated between the collectors and the load. The storage unit is

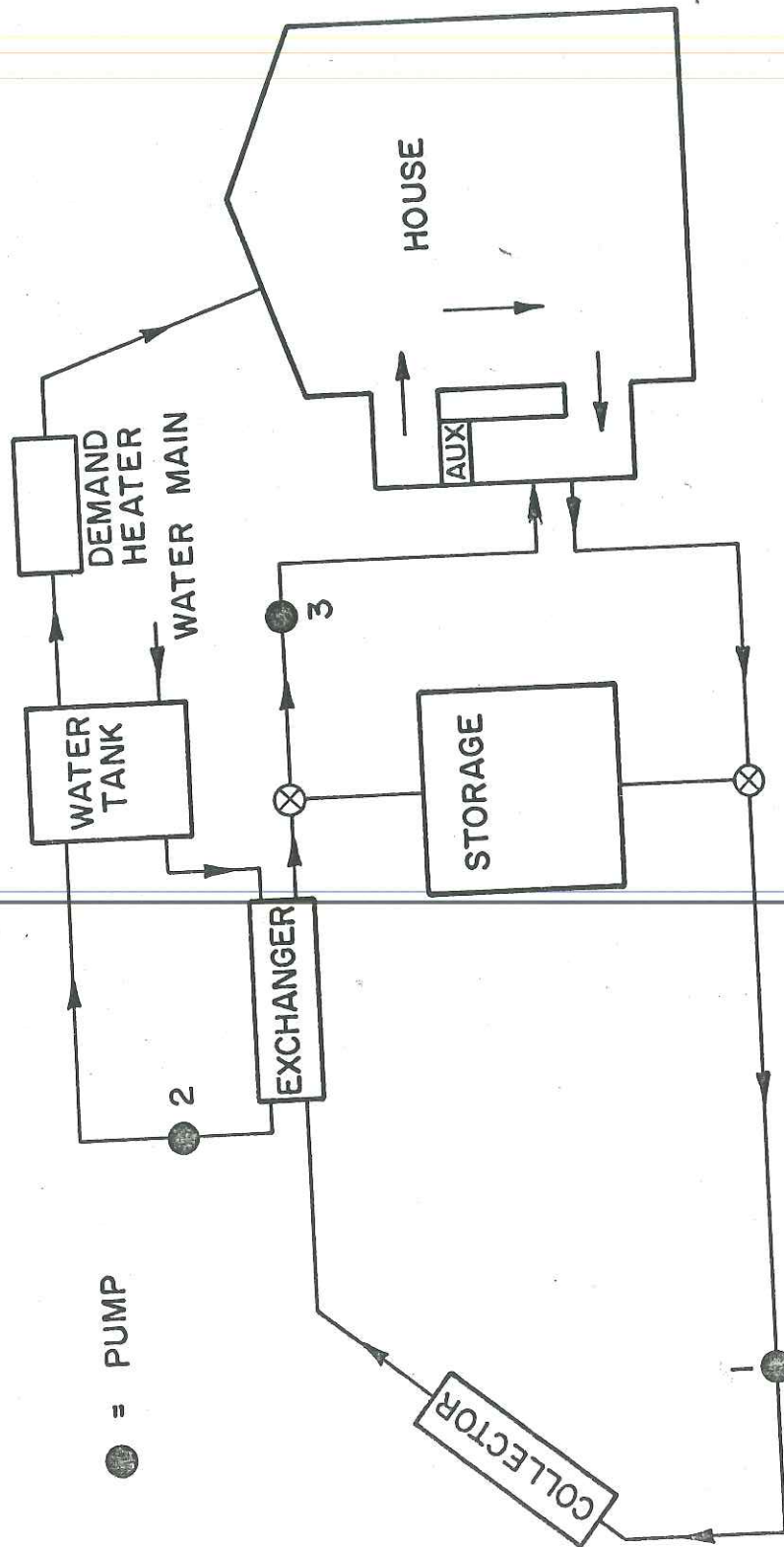


FIGURE 5. Air Based System I.

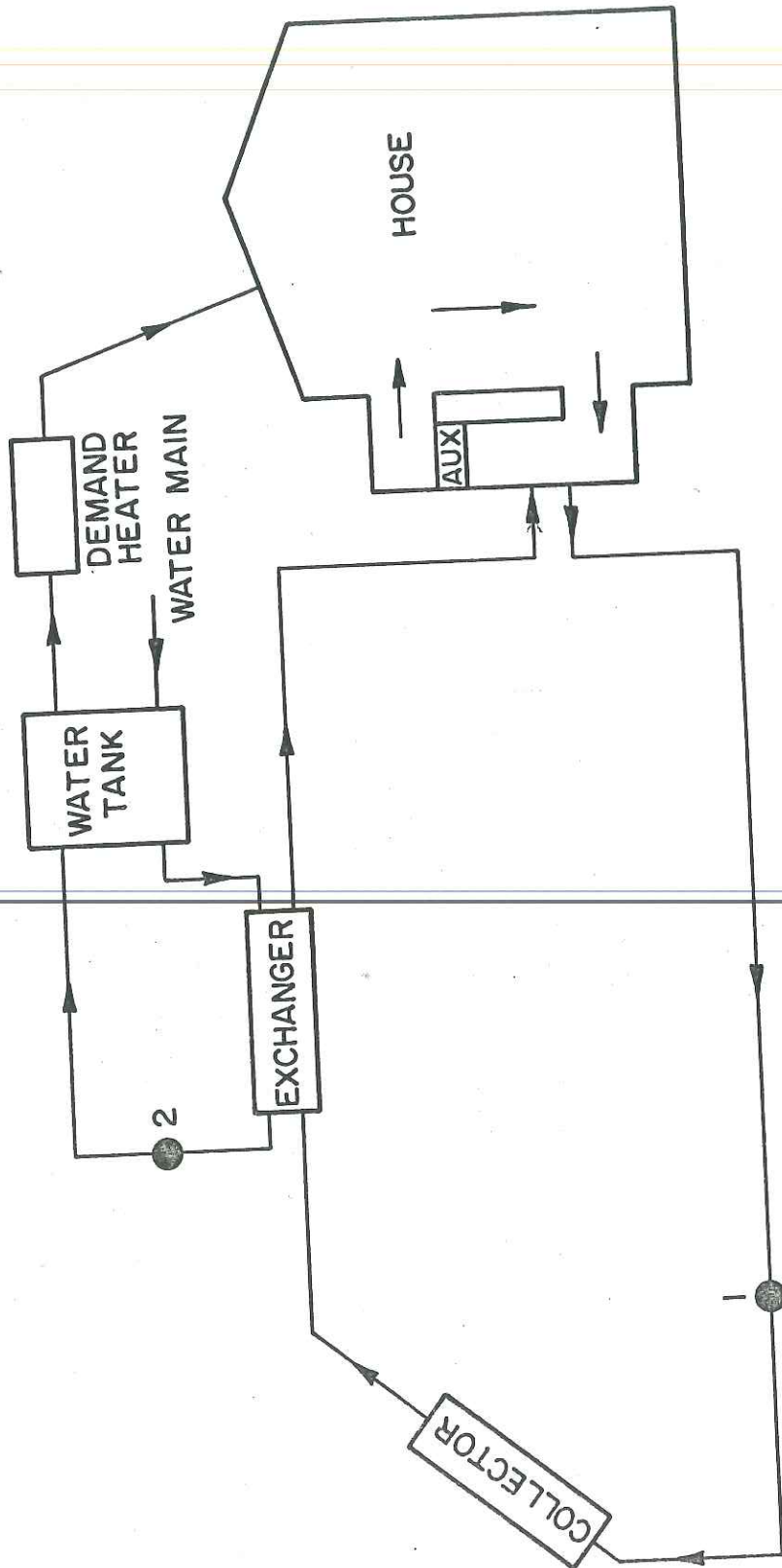


FIGURE 6. Air-Based System II.

TABLE 2  
AIR-BASED SYSTEM PARAMETERS

Collector

1.	collector efficiency factor - $F'$	0.9
2.	fluid thermal capacitance - $C_f$	1.012 KJ/KG °C
3.	collector plate absorptance - $\alpha_p$	.95
4.	number of covers - N	2
5.	collector plate emittance - $\epsilon_p$	.95
6.	loss coefficient for back and edges - $U_{be}$	1.5 KJ/hrm <sup>2</sup> °C
7.	product of extinction coefficient and thickness of each glass cover - KL	.037

Load

1.	heating requirements (energy/degree hr)- UA	1000 KJ/hr°C
2.	load capacitance - $MC_p$	20,000 KJ/°C
3.	constant heat gain - $Q_{gen}$	1,500 KJ/hr

Water preheat tank volume - V .454 m<sup>3</sup>

Air to water cross flow  
heat exchanger effectiveness -  $\epsilon$  .75

Auxiliary space heater capacity -  $Q_{max}$  60,000 KJ/hr

isolated and the conduction mode equations are used. The second mode occurs when solar energy is available for collection and the load is zero. In this case, air is circulated between the collectors and the storage unit. The storage unit is charged and the flow mode equations are used. The final mode occurs when solar energy is not available for collection and the load is not zero. Here, air is circulated between the storage unit and the load. The storage unit is discharged and the flow mode equations are used. During any mode, auxiliary energy may be used to supplement the solar contribution to the load.

The three pumps and two flow diverters in System I are controlled with a two stage thermostat and two on/off differential controllers. The thermostat monitors the room temperature and controls pump 3 and the auxiliary source. It commands first stage (solar source) heating when the room temperature drops below  $21.4\text{ }^{\circ}\text{C}$  ( $70.5\text{ }^{\circ}\text{F}$ ), and second stage (auxiliary source) heating when the room temperature drops below  $18.3\text{ }^{\circ}\text{C}$  ( $64.9\text{ }^{\circ}\text{F}$ ). First stage heating is not disabled during second stage heating unless the solar source temperature is too low.

One on/off differential controller compares the collector outlet air temperature with the preheat water tank temperature and controls pump 2. The other one compares the collector outlet air temperature with the storage unit temperature and controls pump 1.

When both the thermostat and the collector-storage controller are on, the flow diverters direct air from the collectors to the load. When the collector-storage controller is on and the thermostat is off the flow diverters direct air from the collectors to the storage unit. Finally, when the collector controller is off and the thermostat is on, the flow diverters direct air from the storage to the load.

System II has only one operational mode. It occurs when solar energy is available for collection and the load is not zero. Whenever solar energy is not available for collection, or unable to meet the load, the auxiliary source must be used.

System II is controlled with a two stage thermostat and one on/off differential controller. The thermostat monitors the room temperature and controls pump 1 and the auxiliary source. The on/off differential controller compares the collector outlet air temperature with preheat water tank temperature and controls pump 2.

#### 2.4 Results for Air-Based Systems

Air-based systems utilizing two different PCM's were simulated for two locations. Sodium sulfate decahydrate ( $\text{Na}_2\text{SO}_4 \cdot 10\text{H}_2\text{O}$ ) and Sunoco's P116 paraffin wax were selected because they are representative of two different classes of phase change materials: salt hydrates and organic waxes (see Sec. 1.1.1). Madison, (WI) and Albuquerque, (NM) were

the locations chosen since they represent vastly different climates (see Appendix A). Madison is characterized by high heating loads and low amounts of incident solar energy. On the other hand, Albuquerque has almost twice the incident solar energy and only two-thirds the heating load for an identical system.

The variation of the fraction of the load supplied by solar  $\mathcal{F}$  with storage mass and storage/exchanger NTU is shown in Figure 7. These results are intended to show whether the infinite NTU model can adequately describe practical PCES units. They are based on simulations of System I for a two week period in January in Madison. The storage material is paraffin wax (see Table 3 for material properties). The results show that the system performance improves with increasing storage mass and NTU (i.e. higher initial cost). No significant improvement in system performance is realized beyond NTU  $\sim 10$ , which is well within the practical range.<sup>+</sup> Hence, with little error and considerably reduced computational costs, the infinite NTU model can be used to describe practical PCES units. The variation in  $\mathcal{F}$  between the finite

---

<sup>+</sup>The heat exchanger recommended in [6] for paraffin wax has an NTU of approximately 7.5.

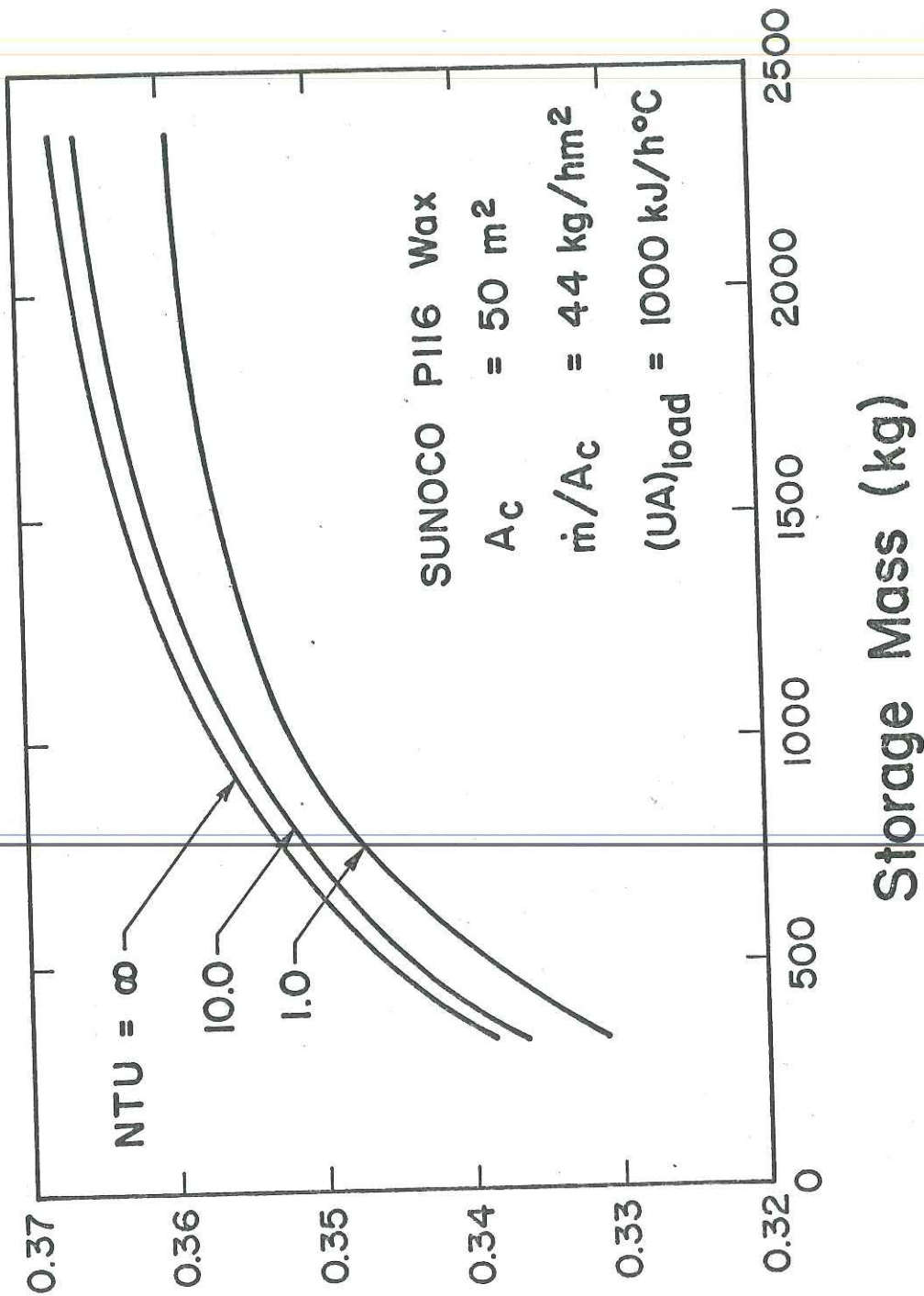


FIGURE 7. Variation of Solar-Supplied Fraction of Load with NTU and Storage Mass for Air-Based Systems Utilizing PCES.

TABLE 3

## PHYSICAL PROPERTIES OF STORAGE MEDIA

<u>Property</u>	<u>Paraffin</u>		
	<u>Wax</u>	<u>Na<sub>2</sub>SO<sub>4</sub>·10H<sub>2</sub>O</u>	<u>Rock</u>
C <sub>S</sub> (KJ/KG°C)	2.89	1.92	0.84
C <sub>ℓ</sub> (KJ/KG°C)	+++	3.26	---
K <sub>S</sub> (KJ/m hr°C)	0.498	1.85	0.45
K <sub>ℓ</sub> (KJ/m hr°C)	+++	Unknown*	---
T* (°C)	46.7	32.0	---
λ (KJ/KG)	209	251	---
ρ <sub>S</sub> (KG/m <sup>3</sup> )	786	1460**	1600
ρ <sub>ℓ</sub> (KG/m <sup>3</sup> )	+++	1330**	---

\*Assumed equal to that for liquid Na<sub>2</sub>HPO<sub>4</sub>·12H<sub>2</sub>O (1714 KJ/mhr°C)

\*\*An average value is used.

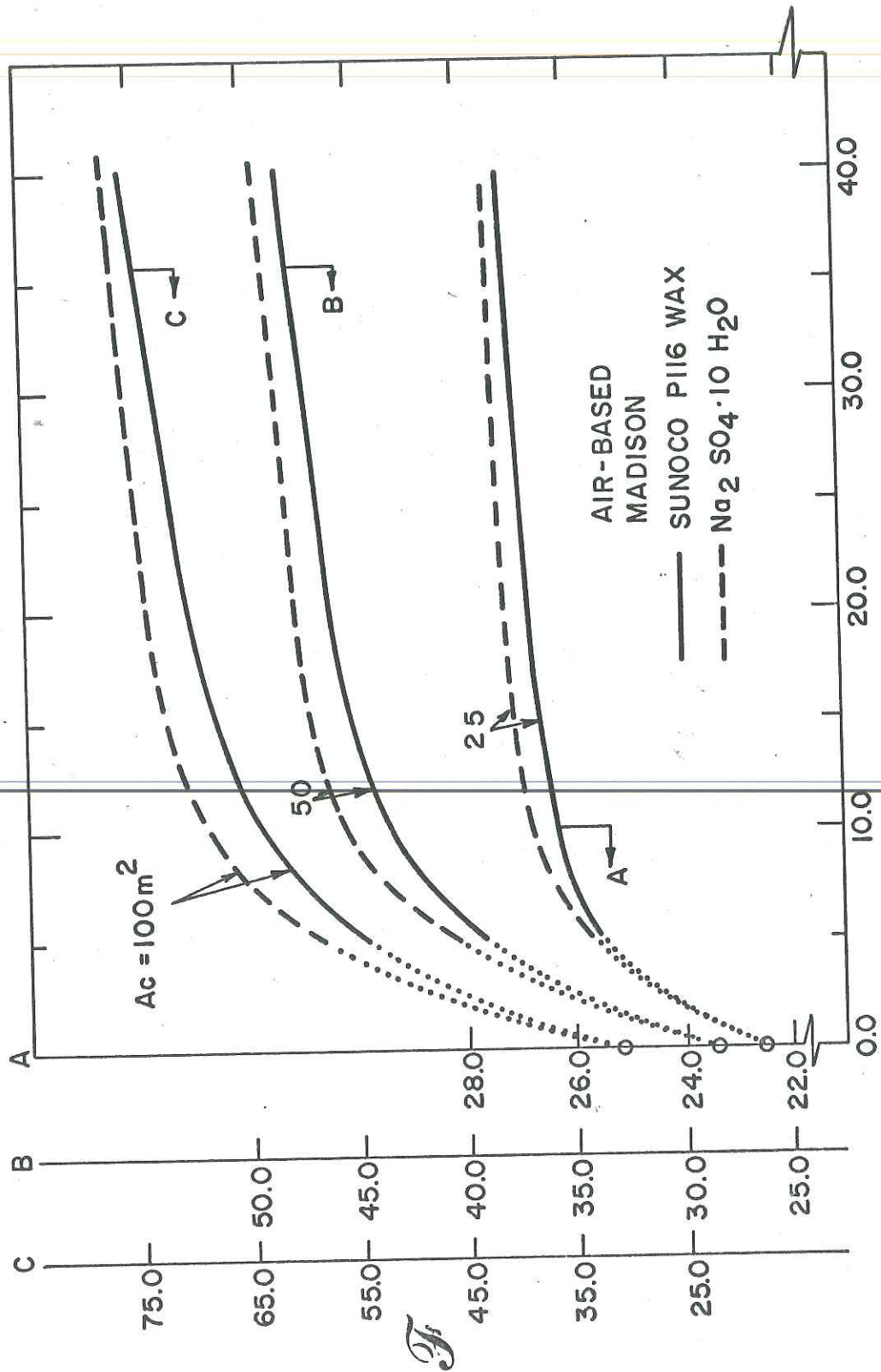
+++Assumed equal to corresponding value for solid phase.

and infinite NTU models will vary under different operating conditions. However, for all practical purposes, the infinite NTU model represents a realistic upper bound to the system performance. All subsequent simulations employ the infinite NTU model.

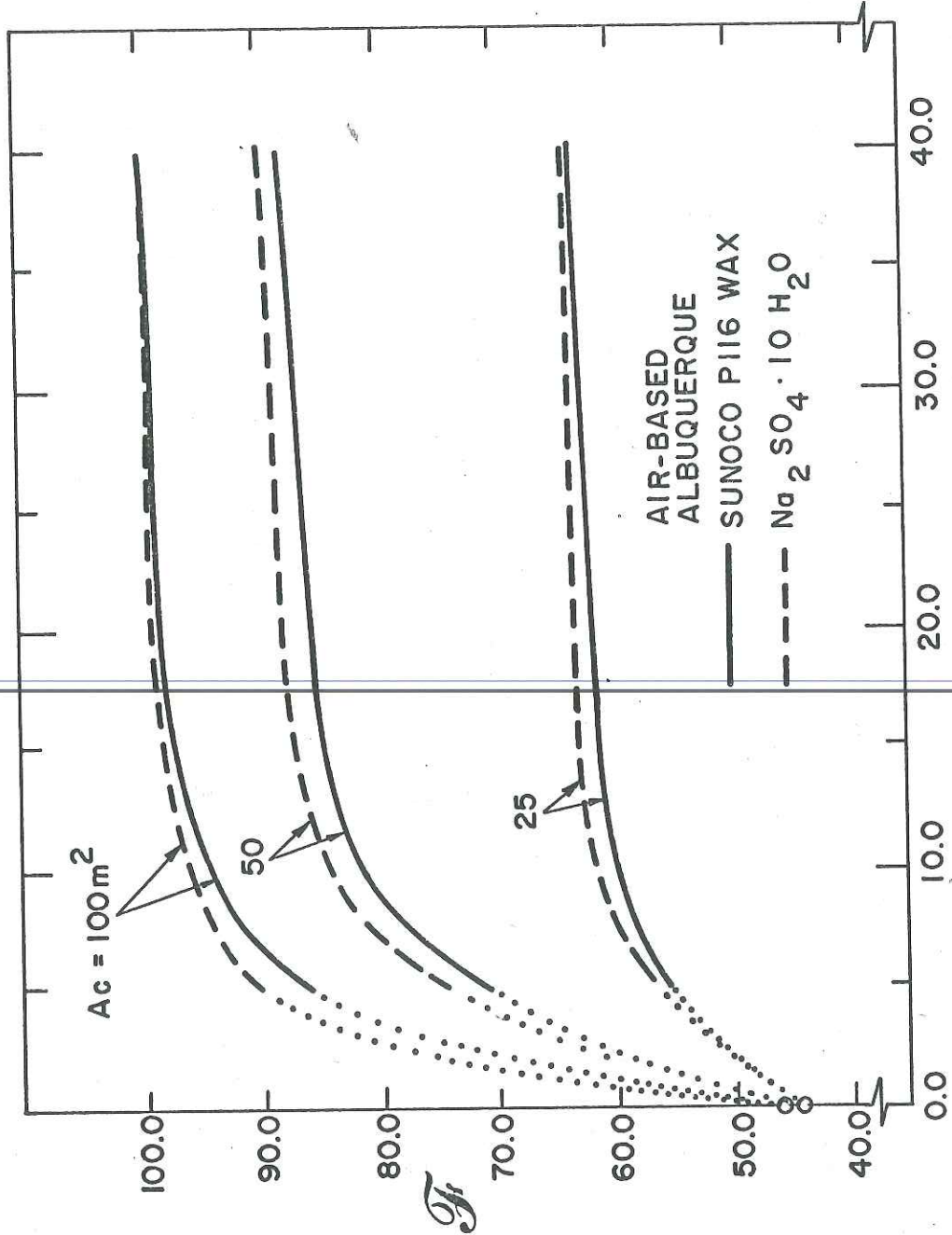
The effect of storage capacity on the long-term performance of air-based systems is shown in Figures 8 and 9 for Madison and Albuquerque respectively. These results are based on a seven month heating season from October 1 to May 1. Collector areas of 25, 50, and 100 square meters were examined for both  $\text{Na}_2\text{SO}_4 \cdot 10 \text{H}_2\text{O}$  and paraffin wax storage units. The simulation of System I generated all the data points except those at storage masses of zero, where System II was used.

Because of the small time steps required and hence, the high computational costs, no data points were generated for systems utilizing extremely small storage capacities. For this reason, the curves in Figure 8 and 9 (and those that follow) are represented by dotted lines in this region to emphasize the uncertainty involved in determining their exact shape.

These figures show that systems utilizing  $\text{Na}_2\text{SO}_4 \cdot 10\text{H}_2\text{O}$  have slightly higher values of  $\mathcal{F}$  than systems utilizing the same mass of paraffin wax. This can be attributed to the lower melting temperature and higher latent heat of the



**STORAGE MASS PER UNIT COLLECTOR AREA ( $\text{kg/m}^2$ )**  
 FIGURE 8. Variation of the Solar-Supplied Fraction of the Load with Storage Mass and Collector Area for Air-Based Systems Utilizing PCES in Madison



### STORAGE MASS PER UNIT COLLECTOR AREA ( $kg/m^2$ )

FIGURE 9. Variation of the Solar-Supplied Fraction of the Load with Storage Mass and Collector Area for Air-Based Systems in Albuquerque.

$\text{Na}_2\text{SO}_4 \cdot 10\text{H}_2\text{O}$ . The isothermal charging of the storage during the phase change will occur at a lower temperature and for a longer duration. This will result in lower collector inlet temperatures and hence, higher collector efficiencies.

Examination of Figures 8 and 9 can yield some insight into the determination of optimum storage capacities. Although the optimum storage capacity will ultimately depend upon the initial and operating costs of the system and the price of auxiliary fuel, a range of values can be recommended based upon the system's thermal performance. In Figure 8 it is clear that in Madison no significant improvement in system performance will be realized for a storage mass per unit collector area greater than  $20\text{KG}/\text{m}^2$  for  $\text{Na}_2\text{SO}_4 \cdot 10\text{H}_2\text{O}$  and  $25\text{ KG}/\text{m}^2$  for paraffin wax. Decreasing the storage capacity below  $7\text{ KG}/\text{m}^2$  for either material will result in a significant drop in system performance.

Figure 9 shows that in Albuquerque increasing the storage mass per unit collector area beyond  $12\text{ KG}/\text{m}^2$  for  $\text{Na}_2\text{SO}_4 \cdot 10\text{H}_2\text{O}$  and  $15\text{ KG}/\text{m}^2$  for paraffin wax will not significantly improve the system's performance. Again, decreasing the storage capacity below about  $7\text{ KG}/\text{m}^2$  will result in a significant drop in system performance.

Therefore, based on system thermal performance, the storage mass per unit collector area for air-based systems should be  $7\text{-}20\text{ KG}/\text{m}^2$  for  $\text{Na}_2\text{SO}_4 \cdot 10\text{H}_2\text{O}$  and  $7\text{-}25\text{ KG}/\text{m}^2$

for paraffin wax. The values in the upper end of the ranges apply to locations characterized by relatively large heating loads and low amounts of incident solar energy (e.g. Madison). As the heating load decreases and the incident solar energy increases (e.g. Albuquerque) the necessary storage size decreases. In either case, economics will dictate the optimum storage size.

The performance of a system utilizing a rock bed storage is shown in Figure 10. This data was generated using the infinite NTU model developed by Hughes et al. [14]. These identical results can also be obtained using the infinite NTU model for PCES. This can be accomplished by setting the material melting temperature  $T^*$  arbitrarily high, so that all energy storage is in the form of sensible heat. In this case, equations 2.15, 2.16 and 1.2 reduce to those given by Hughes et al. [14].

In Figure 11 the performance results for systems utilizing PCES are compared with those utilizing rock bed storage. These results are for systems with 50 square meters of collector area in Madison. It is obvious that sensible and latent heat storage cannot be compared on the basis of a one-to-one correspondence between storage sizes without defining some mean temperature difference. However, a valid comparison can be made over the range of practical storage sizes. Figure 11 shows that, over this range, the rock bed yields a slightly better system performance.

In Figure 12, the data shown in Figure 11 is replotted

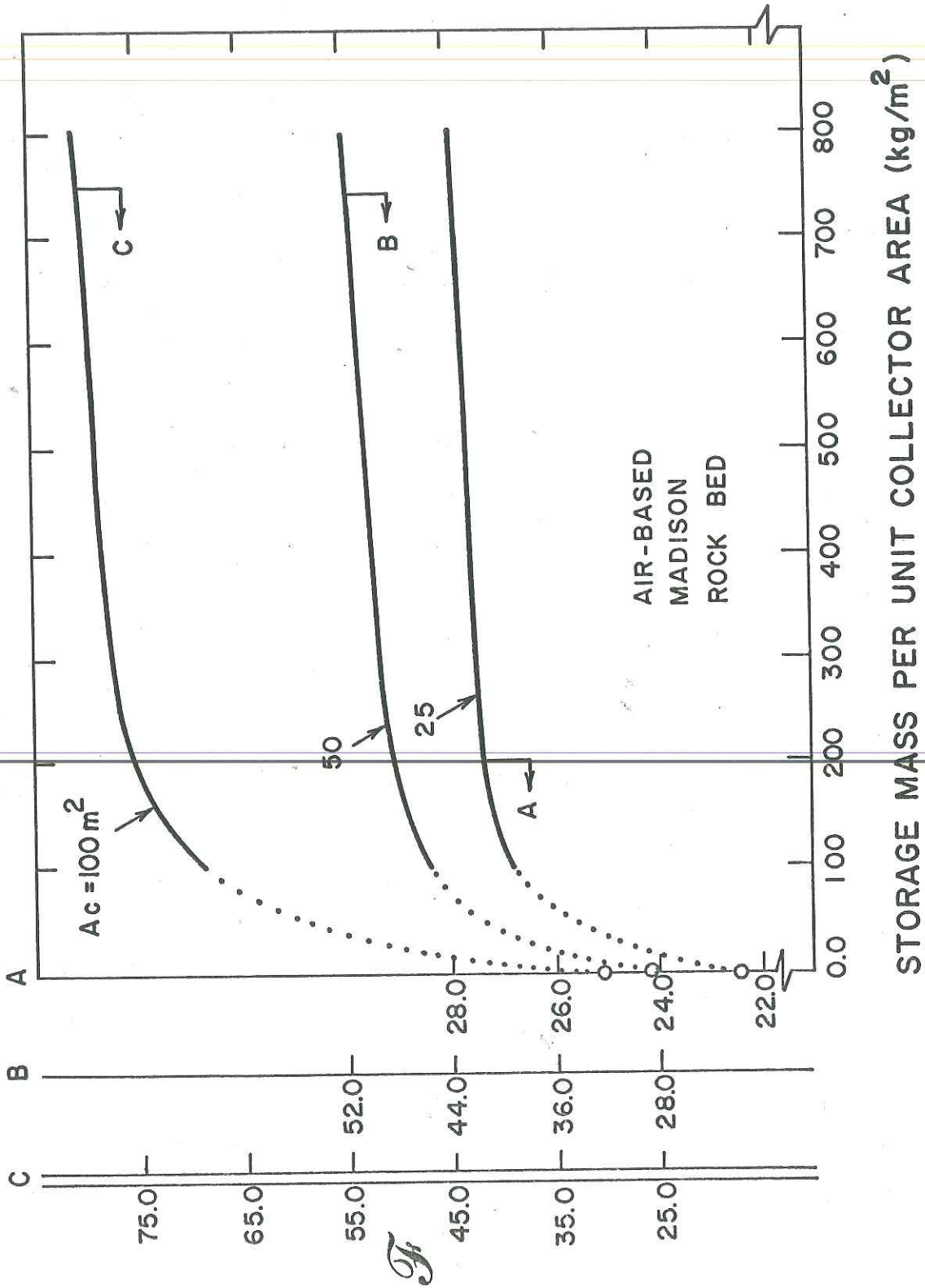


FIGURE 10. Variation of Solar-Supplied Fraction of Load with Storage Mass and Collector Area for Air-Based Systems Utilizing Rock Bed Storage

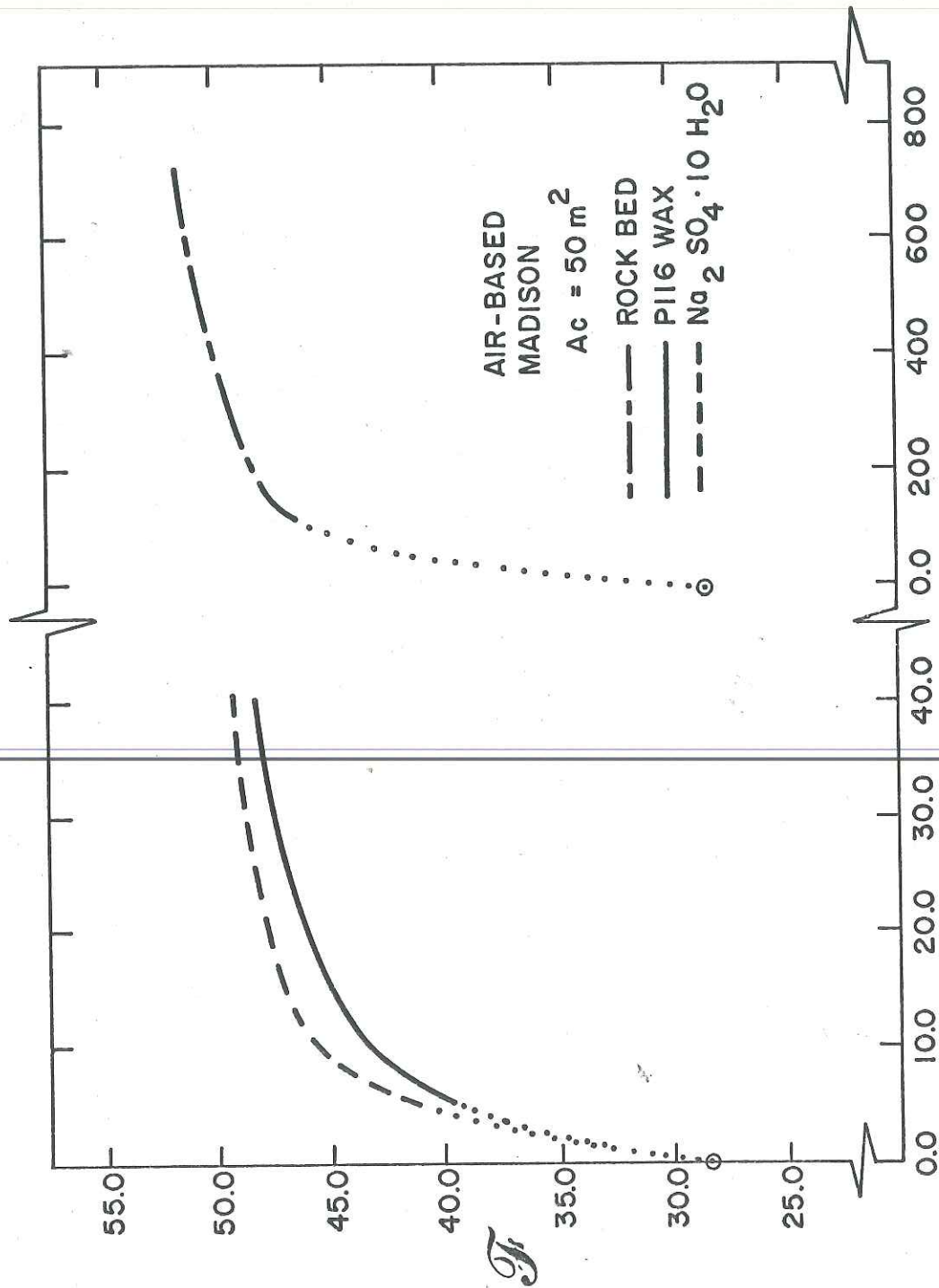


FIGURE 11. Variation of Solar-Supplied Fraction of Load with Storage Mass for Air-Based System Utilizing Sensible and Latent Heat Storage Media in Madison.

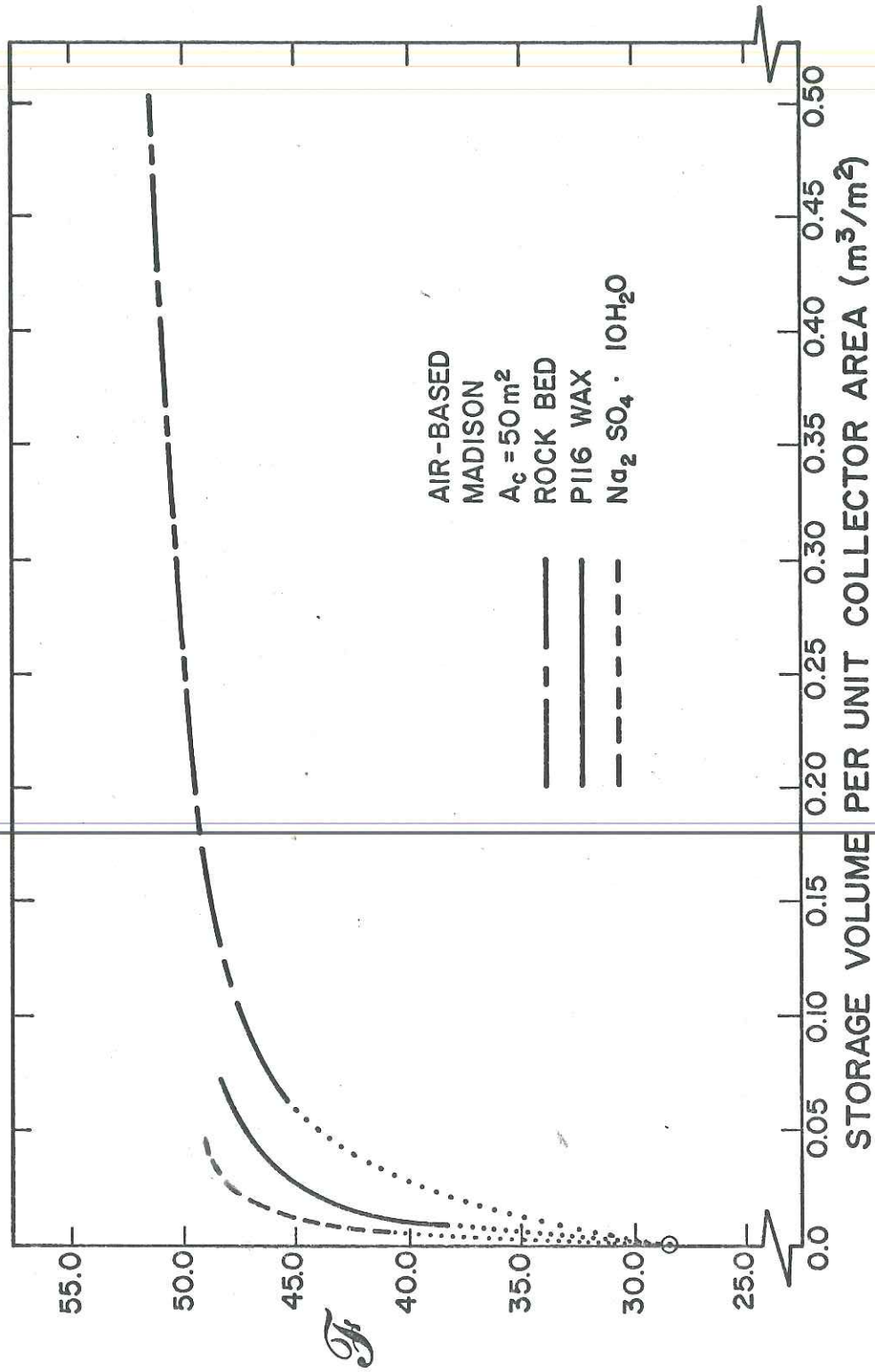


FIGURE 12. Variation of Solar-Supplied Fraction of Load with Storage Volume for Air-Based Systems Utilizing Sensible and Latent Heat Storage Media in Madison.

in terms of storage volume per unit collector area. Although the curves are distorted, they serve to illustrate the savings in storage volume that can be achieved with PCES compared to rock bed storage. For example, an  $F$  value of 47.5 will be realized by a system utilizing either  $\text{Na}_2\text{SO}_4 \cdot 10\text{H}_2\text{O}$  with a storage volume of 0.024 cubic meters per unit collector area (20  $\text{Kg}/\text{m}^2$ ), paraffin wax with a storage volume of 0.052 cubic meters per unit collector area (25  $\text{Kg}/\text{m}^2$ ), or a rock bed with a storage volume of 0.110 cubic meters per unit collector area. This means that a system utilizing  $\text{Na}_2\text{SO}_4 \cdot 10\text{H}_2\text{O}$  will require roughly one-fourth the storage volume of a rock bed system in order to achieve the same system performance. A system utilizing paraffin wax will require only one-half the storage volume of a rock bed system in order to realize the same system performance.

In Figure 13 the comparison between sensible and latent heat storage is shown for Albuquerque. Here again, the rock bed system appears to perform slightly better than the PCES system.

In Figure 14 the results of Figure 13 for Albuquerque are replotted in terms of storage volume per unit collector area. As was the case for Madison, systems utilizing PCES will require significantly smaller storage volumes than those with a rock bed. For example, systems with either 0.014 cubic meters per unit collector area of  $\text{Na}_2\text{SO}_4 \cdot 10 \text{H}_2\text{O}$  (12  $\text{Kg}/\text{m}^2$ ), 0.027 cubic meters per unit collector area of paraffin

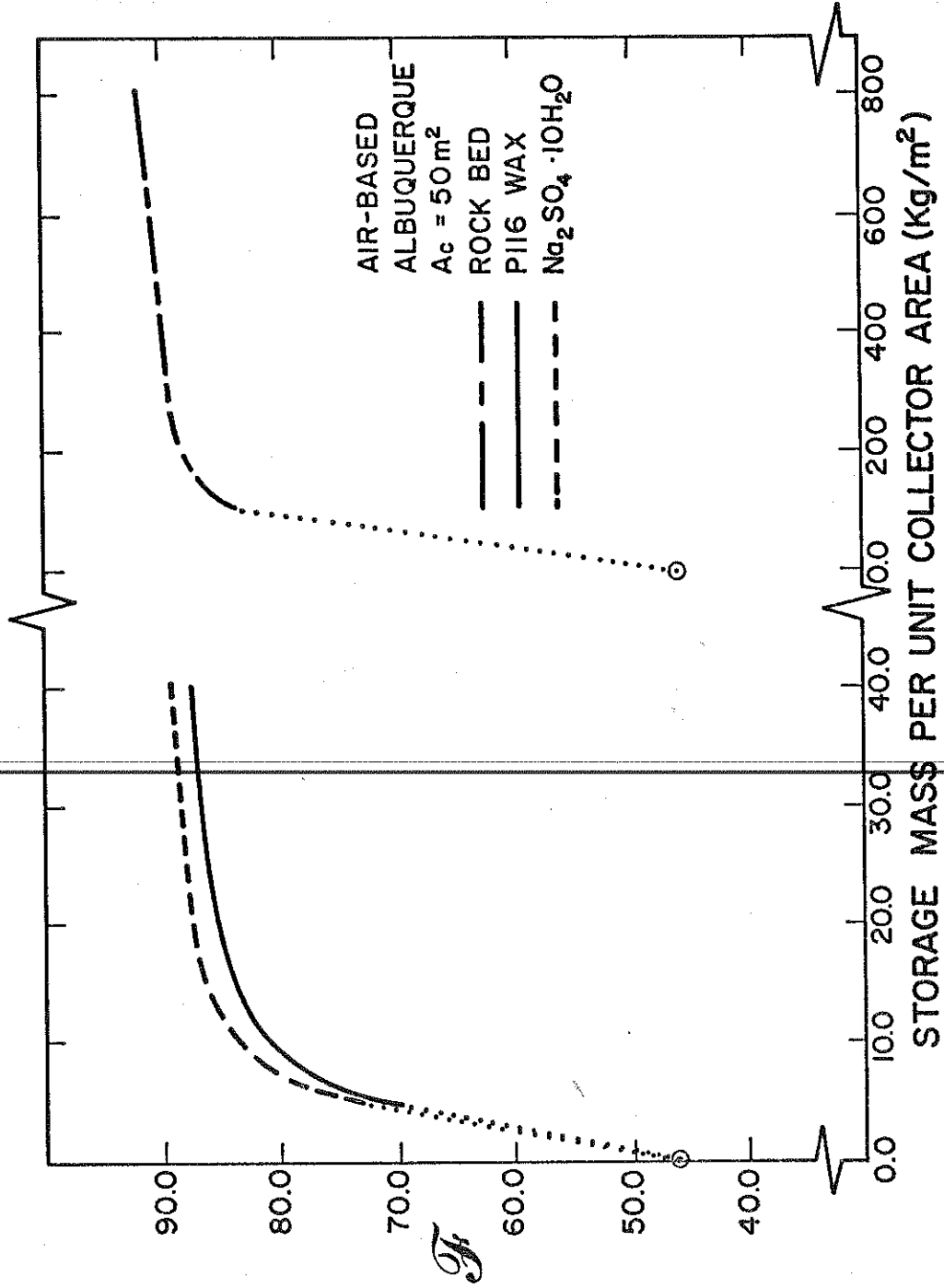


FIGURE 13. Variation of Solar-Supplied Fraction of Load with Storage Mass for Air-Based Systems Utilizing Sensible and Latent Heat Storage Media in Albuquerque.

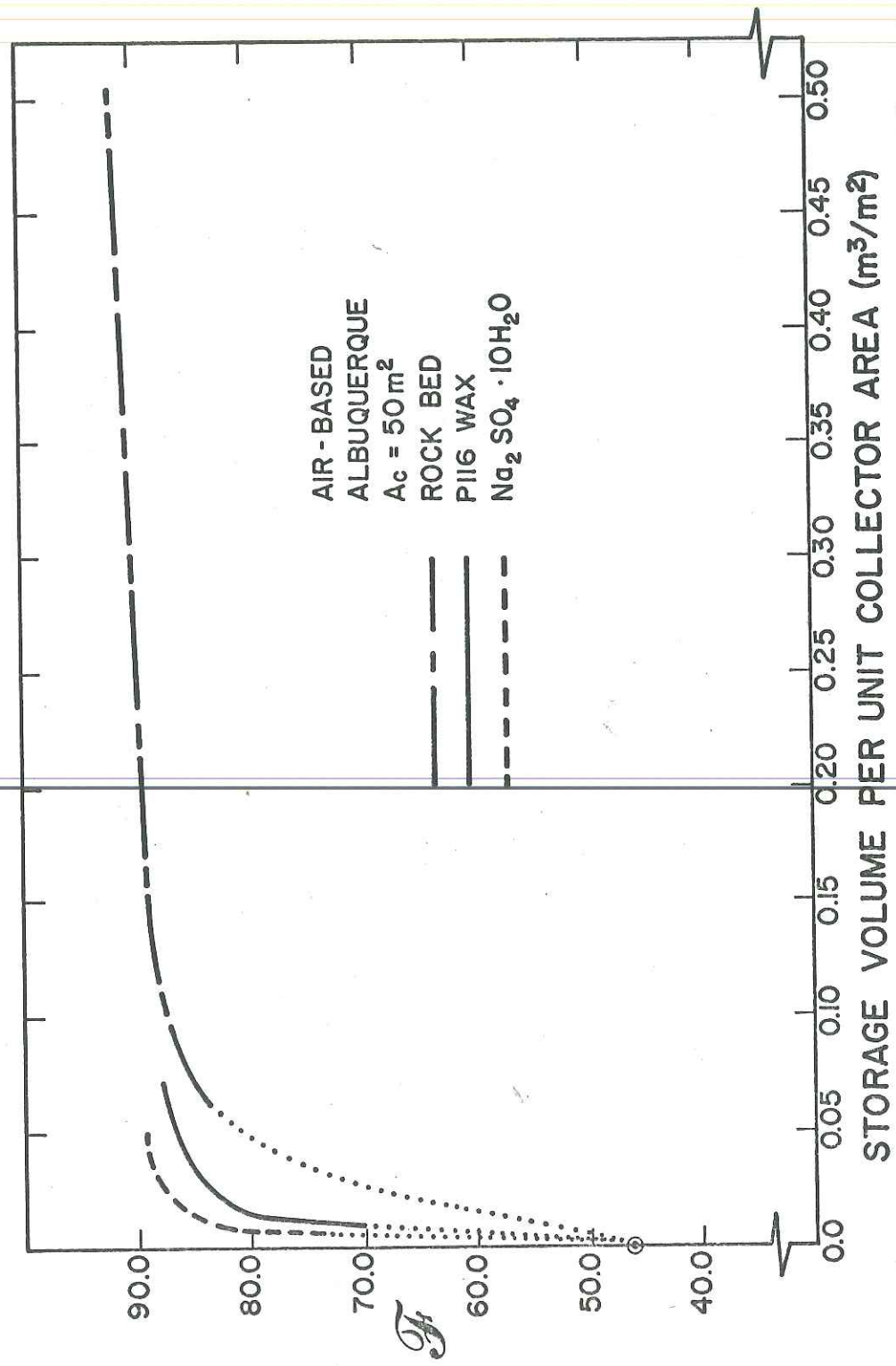


FIGURE 14. Variation of Solar-Supplied Fraction of Load with Storage Volume for Air-Based Systems Utilizing Sensible and Latent Heat Storage Media in Albuquerque.

wax ( $15 \text{ kg/m}^2$ ), or 0.060 cubic meters per unit collector area of rock bed will have  $\mathcal{F}$  values of 82.2. Hence, the "savings ratios" for Albuquerque are roughly the same as those for Madison. Systems utilizing  $\text{Na}_2 \text{SO}_4 \cdot 10 \text{ H}_2\text{O}$  will require only one-fourth the storage volume of a rock bed in order to realize the same system performance. Systems utilizing paraffin wax will require one-half the storage volume of a rock bed in order to yield the same system performance.

Figure 15 shows the effect of storage capacity on collector efficiency  $\eta_c$ . Collector efficiency is defined as the useful energy collected divided by the total incident solar energy. The fraction of the load supplied by solar  $\mathcal{F}$  is defined as the total load minus the total auxiliary supplied (i.e. the useful energy collected) divided by the total load. These quantities differ only in their denominators which are constants. Hence, Figure 15 presents the same comparison between storage types as Figures 11 and 13, but in a slightly different manner.

Another parameter of interest in these simulations is the fraction of time,  $\phi$ , that any or all of the storage material is in the two-phase region. In Madison, for paraffin wax, this fraction ranged from 10 to 64%; for  $\text{Na}_2\text{SO}_4 \cdot 10\text{H}_2\text{O}$  it varied between 11 and 74%. In Albuquerque the values were 36 to 99% for the wax and 41 to 99% for the  $\text{Na}_2\text{SO}_4 \cdot 10\text{H}_2\text{O}$ . The exact value is dependent upon the storage size and the collector area. The higher values correspond to the larger

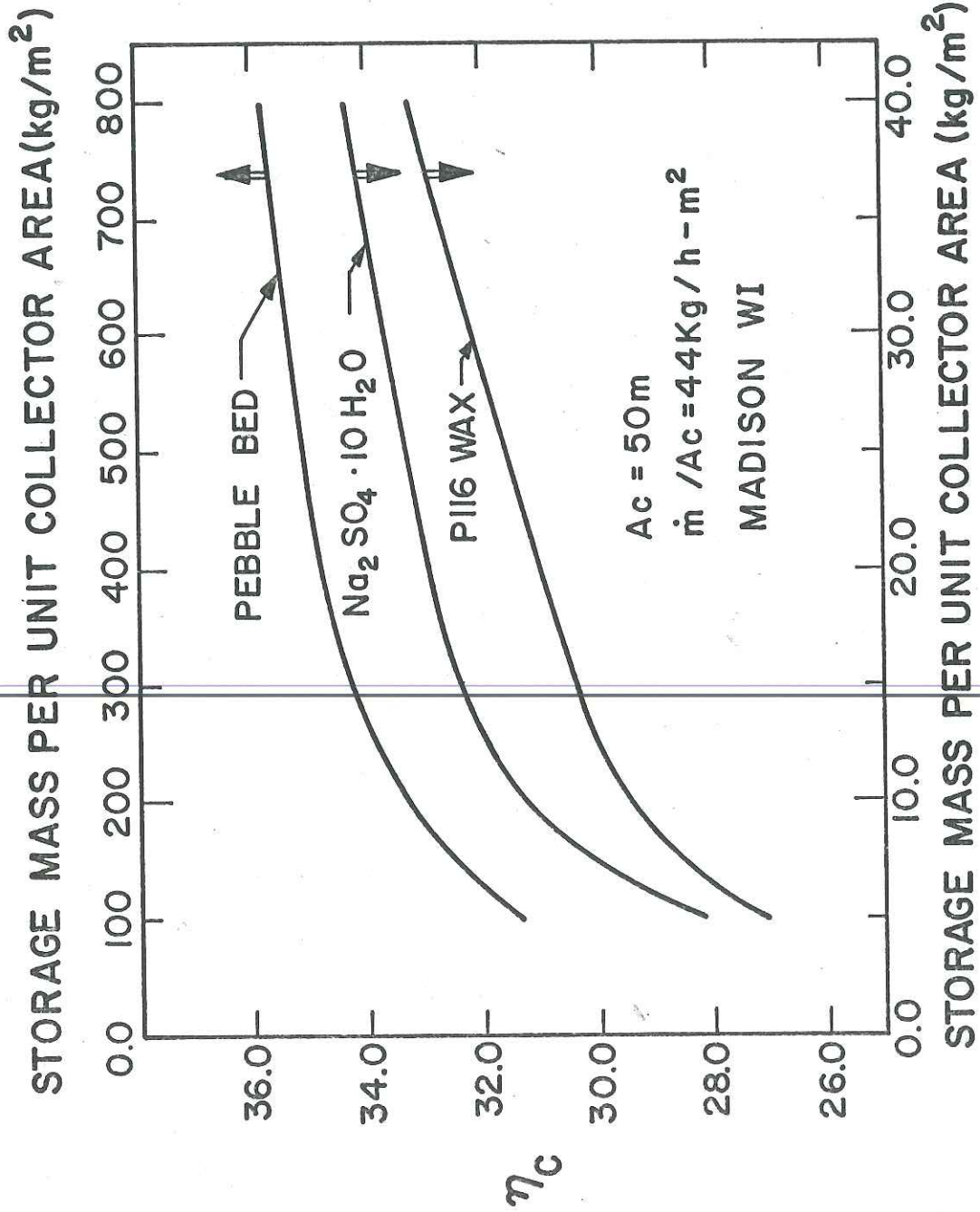


FIGURE 15. Variation of Collector Efficiency with Storage Mass for Air-Based Systems Utilizing Sensible and Latent Heat Storage Media.

collector areas as is illustrated in Figure 16 for Madison.

The effect of the collector loss characteristics on the relative performance of sensible and latent heat storage is shown in Figure 17. The low loss collector used in these simulations had a plate absorptance of 0.95, an emittance of 0.15, two glass covers and a bottom and edge loss coefficient of  $1.5 \text{ KG/hr m}^2\text{°C}$ . The high loss collector had a plate absorptance of 0.95, an emittance of 0.95, one cover and a bottom and edge loss coefficient of  $2.5 \text{ KG/hr m}^2\text{°C}$ .

These results show that, although the low loss collector performs considerably better than high loss collector, the difference in results between the high loss and low loss collectors is the same for both types of storage. Therefore, the comparisons presented earlier between sensible and latent heat storage seem to hold regardless of the "quality" of the collectors used.

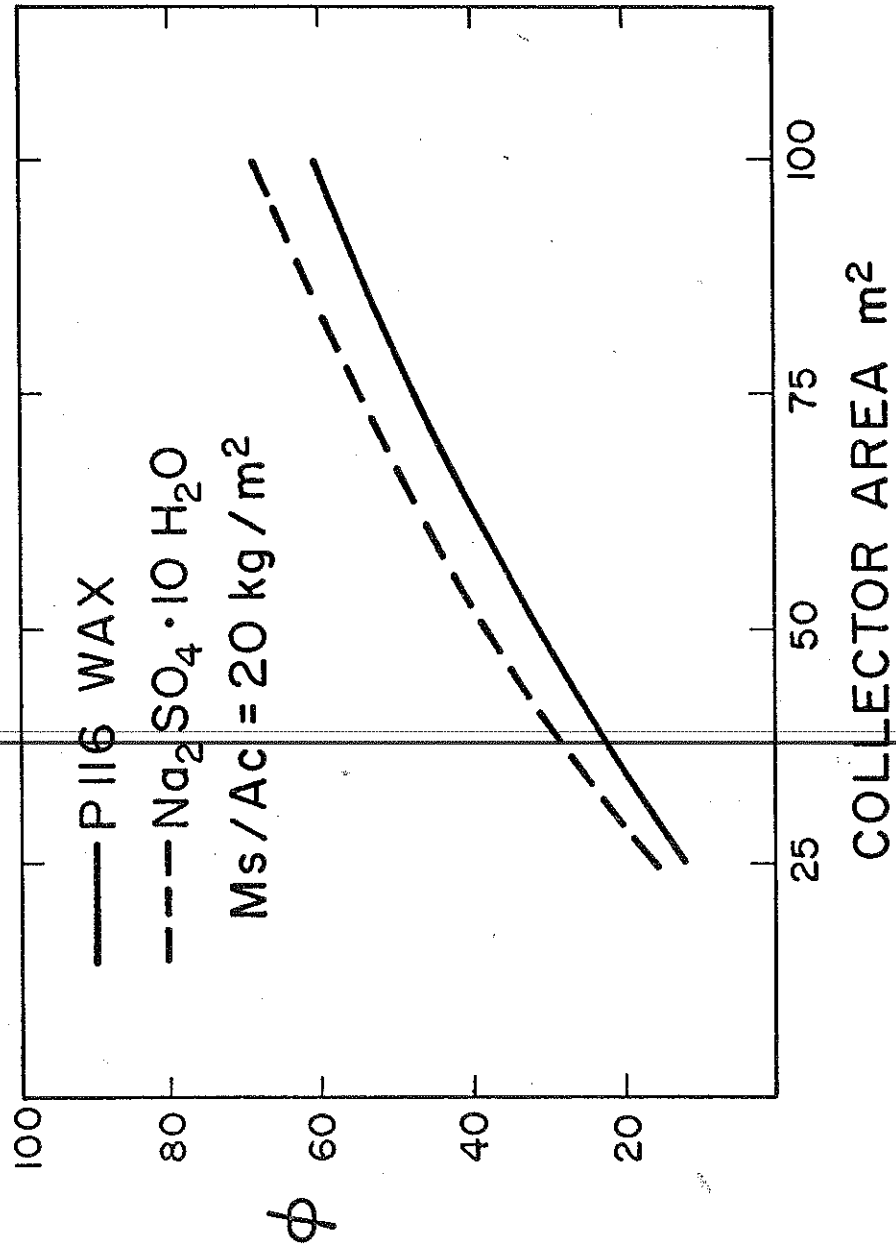
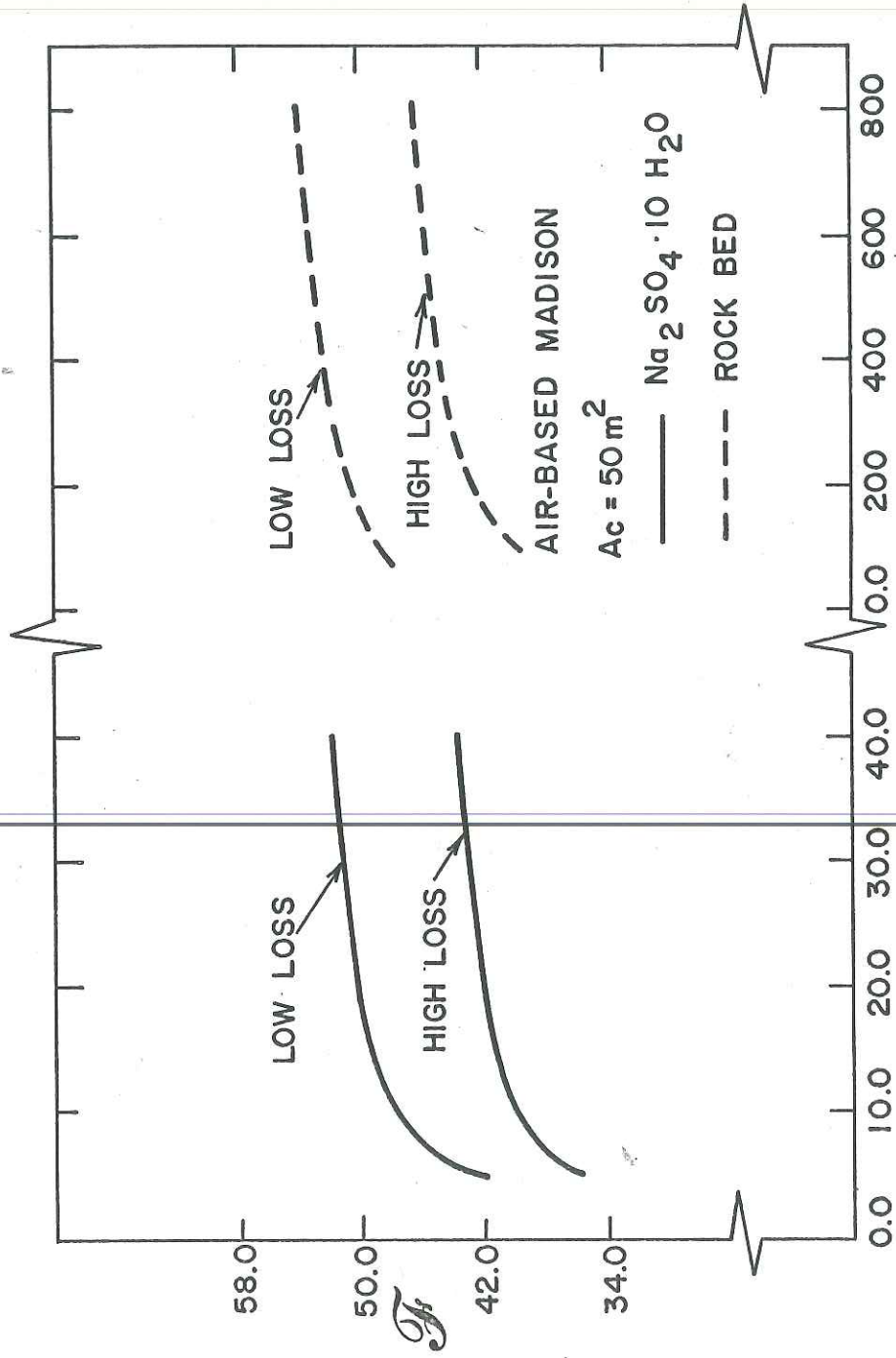


FIGURE 16. Variation of the Fraction of Heating Season PCM Spends in Liquid State with Collector Area.



STORAGE MASS PER UNIT COLLECTOR AREA ( $\text{kg}/\text{m}^2$ )

FIGURE 17. Effect of Collector "Quality" on Performance of Air-Based Systems Utilizing Sensible and Latent Heat Storage Media.

## CHAPTER 3

## PERFORMANCE OF LIQUID-BASED SYSTEMS UTILIZING PCES

Section 1 of this chapter describes the three models developed in this investigation for use in the simulation of liquid-based systems. Section 2 explains the method of solution. Section 3 contains the configurations and control strategies for the systems simulated. The results for liquid-based systems are given in section 4.

### 3.1 Modeling PCES for Liquid-Based Systems

The first PCES model developed for use in the simulation of liquid-based systems is almost identical to the general model described earlier (i.e. equations 1.1 - 1.5 for the flow modes and 1.1 - 1.3, 2.1 and 2.2 for the conduction mode). The only difference is that axial conduction in the PCM during the flow modes is neglected. For the sake of continuity, this version is outlined below.

The following assumptions are made:

1. Neglect differences between the physical properties of the liquid and solid phases of the PCM.
2. Neglect axial conduction in the circulating fluid and the PCM in the flow modes.
3. The Biot number is sufficiently low such that temperature variations normal to flow direction can be ignored.

4. Neglect heat losses to the surroundings.

Flow Mode: The governing equations and boundary conditions for the PCM are:

$$\frac{\partial u}{\partial t} = \frac{UP}{\rho A} (T_f - T) \quad (3.1)$$

and

$$\begin{aligned} \frac{\partial T}{\partial z} \Big|_{z=0} &= 0 \\ \frac{\partial T}{\partial z} \Big|_{z=l} &= 0 \end{aligned} \quad (1.3)$$

For the circulating fluid, the governing equations and boundary conditions are:

$$\frac{\partial T_f}{\partial t} = \frac{UP}{\rho_f A_f c_f} (T - T_f) - \frac{\dot{m}}{\rho_f A_f} \frac{\partial T_f}{\partial z} \quad (1.4)$$

and

$$T_f(0, t) = f(t) \quad (1.5)$$

Conduction Mode: The boundary conditions for the PCM are the same as those for the flow mode. The governing equation for the PCM is now:

$$\frac{\partial u}{\partial t} = \frac{K}{\rho} \frac{\partial^2 T}{\partial z^2} + \frac{U'P}{\rho A} (T_f - T) \quad (1.1)$$

For the circulating fluid, the governing equation and boundary conditions are:

$$\frac{\partial T_f}{\partial t} = \frac{K_f}{c_f \rho_f} \frac{\partial^2 T_f}{\partial z^2} + \frac{U'P}{\rho_f A_f c_f} (T - T_f) \quad (2.1)$$

and

$$\begin{aligned} \frac{\partial T_f}{\partial z} \Big|_{z=0} &= 0 \\ \frac{\partial T_f}{\partial z} \Big|_{z=l} &= 0 \end{aligned} \quad (2.2)$$

The specific internal energy  $u$  is related to the temperature  $T$  and liquid fraction  $\chi$  as follows:

$$u = c(T - T_{ref}) + \chi\lambda$$

$$\begin{array}{lll} \text{for} & T < T^* & \chi = 0 \\ \text{for} & T = T^* & 0 \leq \chi \leq 1 \\ \text{for} & T > T^* & \chi = 1 \end{array} \quad (1.2)$$

### 3.1.1 Infinite NTU Model for Liquid-Based Systems

As indicated in the previous chapter, the modeling of PCES can be simplified and the computational costs considerably reduced if it is assumed that the storage unit has an NTU of infinity. The results of the investigation of air-based systems showed that an infinite NTU model can adequately describe practical PCES units (see Figure 8). The governing equations that result from the addition of this assumption to the liquid-based model are given below.

The boundary conditions remain unchanged.

Flow Mode: Governing equations 3.1 and 1.4 for the PCM and circulating fluid can be combined to yield the following:

$$\frac{\partial u}{\partial t} = -\frac{C_f \dot{m}}{\rho A} \frac{\partial T_f}{\partial z} - \frac{\rho_f A_f C_f}{\rho A} \frac{\partial T_f}{\partial t} \quad (3.2)$$

When the NTU is infinite, the PCM and circulating fluid temperatures at any axial position in the storage unit will be identical. Hence, equation 3.2 can be rewritten as:

$$\frac{\partial u}{\partial t} + \frac{\rho_f A_f C_f}{\rho A} \frac{\partial T}{\partial t} = -\frac{c_f \dot{m}}{\rho A} \frac{\partial T}{\partial z} \quad (3.3)$$

The solution of equation 3.3 can be made considerably easier by the introduction of a new variable  $\psi$  which is defined as:

$$\psi = u + \frac{\rho_f A_f C_f}{\rho A} T \quad (3.4)$$

Because they are at the same temperatures, the "specific" internal energy of both the PCM and the circulating fluid can be represented by the single variable  $\psi$ .

The governing equations for the flow mode become:

$$\frac{\partial \psi}{\partial t} = -\frac{\dot{m} c_f}{\rho A} \frac{\partial T}{\partial z} \quad (3.5)$$

and

$$T_f = T \quad (3.6)$$

Conduction Mode: The governing equations 1.1 and 2.1 for the PCM and circulating fluid can be combined as follows:

$$\frac{\partial u}{\partial t} = \frac{K}{\rho} \frac{\partial^2 T}{\partial z^2} - \frac{\rho_f A_f C_f}{\rho A} \frac{\partial T_f}{\partial t} + \frac{K_f A_f}{\rho A} \frac{\partial^2 T_f}{\partial z^2} \quad (3.7)$$

Again, the PCM and circulating fluid temperatures are the same so that upon introducing the variable  $\psi$  the governing equations for the conduction mode become:

$$\frac{\partial \psi}{\partial t} = \left( \frac{K}{\rho} + \frac{K_f A_f}{\rho A} \right) \frac{\partial^2 T}{\partial z^2} \quad (3.8)$$

and

$$T_f = T \quad (3.9)$$

An equation relating  $\psi$ ,  $T$ , and  $\chi$  can be obtained by combining equation 1.2 with the definition of  $\psi$  (equation 3.4) to yield:

$$\psi = c (T - T_{ref}) + \chi \lambda + \frac{\rho_f A_f C_f}{\rho A} T \quad (3.10)$$

$$\begin{array}{lll} \text{for } T < T^* & \chi = 0 \\ \text{for } T = T^* & 0 \leq \chi \leq 1 \\ \text{for } T > T^* & \chi = 1 \end{array}$$

### 3.1.2 Variable Properties

If there is a significant variation in the PCM thermal conductivity between the solid and liquid phases it can be accounted for as shown in chapter two (see equation 2.17). In order to account for variations in the PCM specific heat, equation 3.10 can be modified as follows:

$$\begin{aligned} \psi &= c_s (T - T_{ref}) + \frac{\rho_f A_f C_f}{\rho A} T && \text{for } T < T^* \\ \psi &= c_s (T^* - T_{ref}) + \frac{\rho_f A_f C_f}{\rho A} T^* + \chi \lambda && \text{for } T = T^* \\ \psi &= c_s (T^* - T_{ref}) + \frac{\rho_f A_f C_f}{\rho A} T + \lambda + c_l (T - T_{ref}) && \text{for } T > T^* \end{aligned} \quad (3.11)$$

### 3.2 Method of Solution

The finite differencing scheme and the stability and accuracy criteria employed in the simulation of liquid-based systems are similar to those described in chapter two for air-based systems. Here again, computer programs compatible with the requirements of TRNSYS [15] were written for each of the three PCES models, viz. the finite NTU (general) model, the infinite NTU model, and the variable properties model.

### 3.3 Liquid-Based System Description and Control Strategy

The three liquid-based systems simulated in this investigation are shown in Figures 18, 19, and 20. System I is the configuration designed to utilize PCES. System II is a standard liquid-based system incorporating a conventional water tank. System III is the same as System I except that it has no storage capability. The parameters selected for liquid-based system components are identical to those shown in Table 2 for air-based systems except for the circulating fluid capacitance; in this case the values are 4.19 KJ/Kg°C for water and 3.35 KJ/Kg°C for a 1:1 water/ethylene glycol mixture.

System I is a "hybrid" system in that it is a combination of the standard air-based system (Figure 5) and the

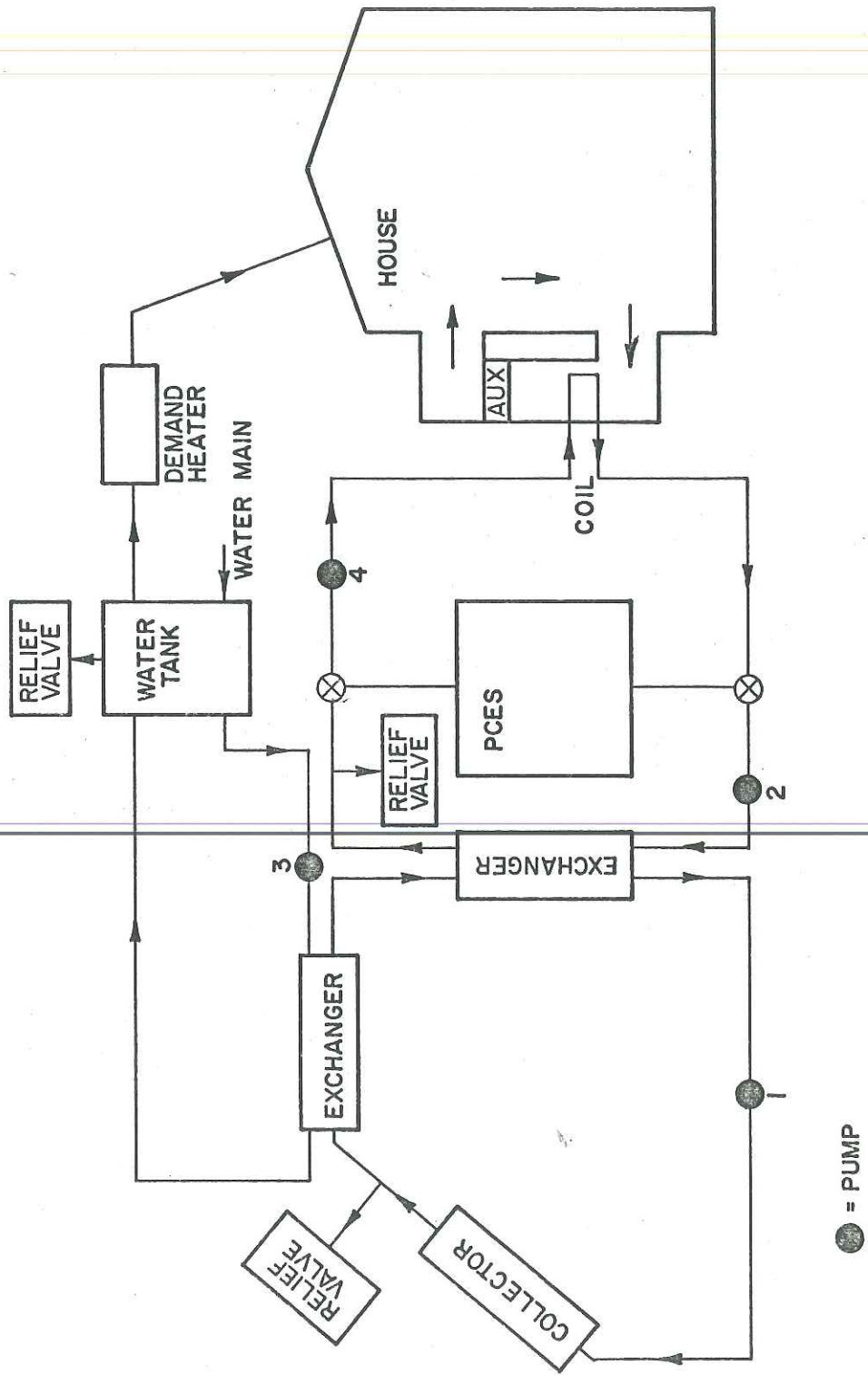


FIGURE 18. Liquid-Based System I.

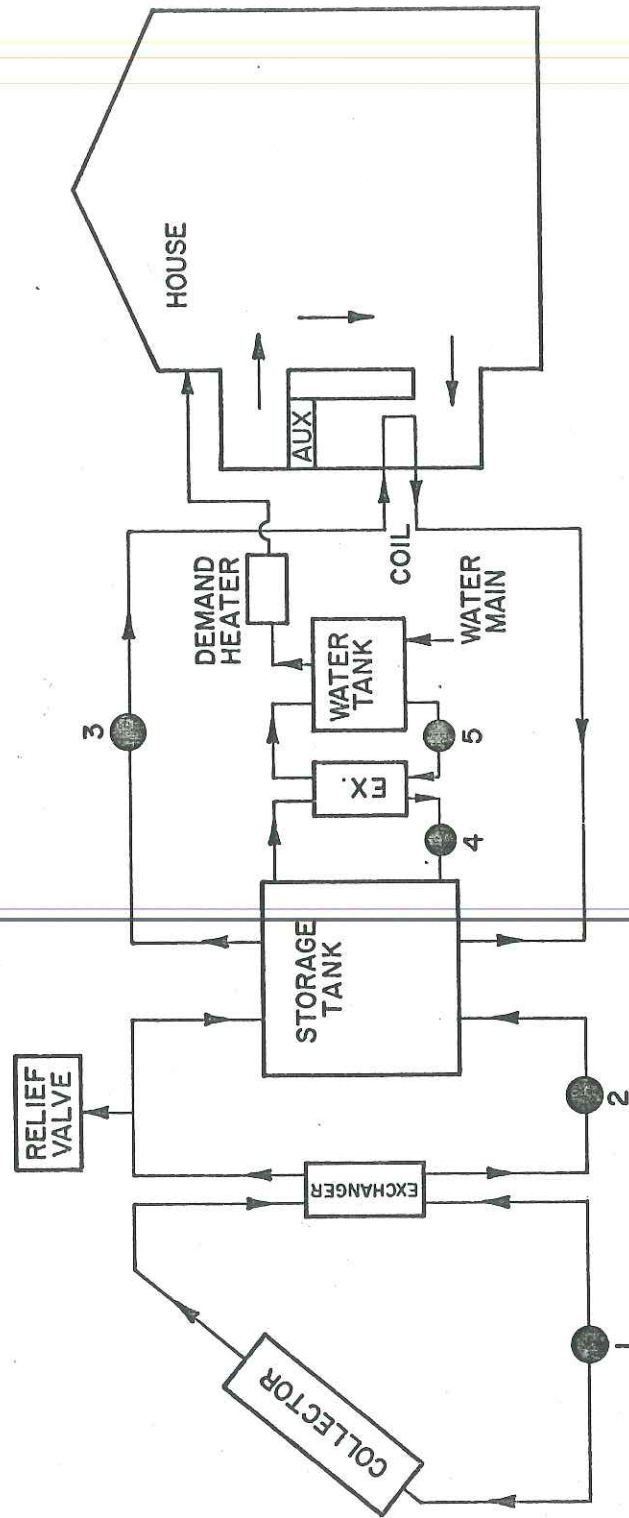


FIGURE 19. Liquid-Based System II.

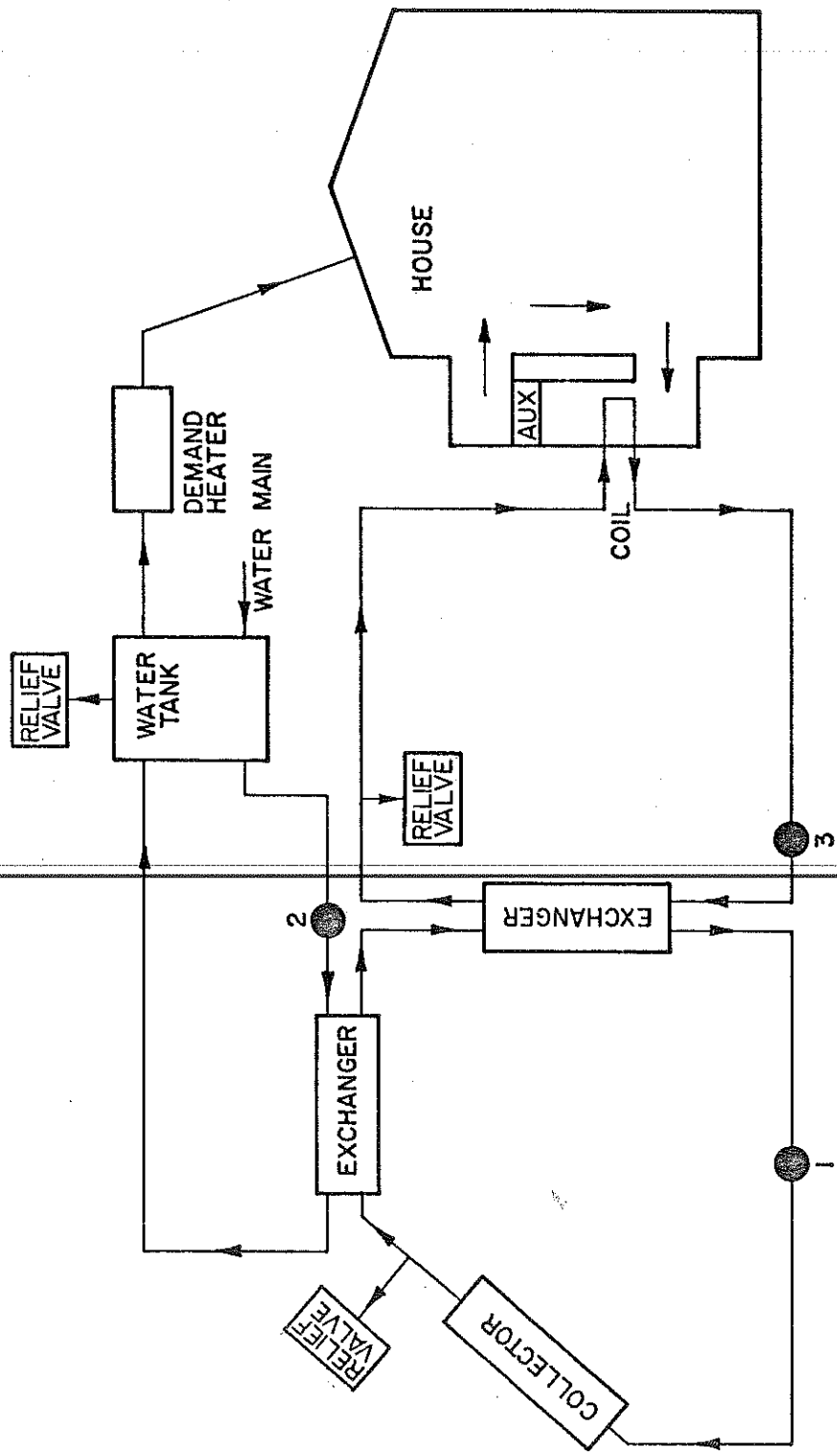


FIGURE 20. Liquid-Based System III.

standard liquid-based system (Figure 19). It is similar to the standard air-based system in that the circulating fluid can move through the storage unit in only one direction at a time to facilitate either charging or discharging (not both simultaneously). Also, the domestic preheat water tank is supplied from a collector loop heat exchanger instead of from the main storage unit. On the other hand, System I is similar to the standard liquid-based system in that the collector is contained in a loop (with a water/ethylene glycol mixture for a circulating fluid) isolated from the rest of the system by heat exchangers.

Liquid-based System I has the same basic operational modes as the air-based System I. If solar energy is available for collection, it can be supplied to the space heating load (mode 1) or to the storage unit (mode 2). If solar energy is not available and the space heating load is not zero, it is met by the storage unit (mode 3). Auxiliary energy can be used to supplement the solar contribution to the load during any of these modes.

The four pumps and two flow diverters in System I are controlled by a two stage thermostat and two on/off differential controllers. The thermostat monitors room temperature and controls pump 4 and the auxiliary energy source. One on/off controller monitors the collector outlet temperature and the storage unit temperature and controls

pumps 1 and 2. The other on/off controller monitors the collector outlet temperature and the preheat water tank temperature and controls pumps 1 and 3 (pump 1 can be turned on by either controller).

If both the thermostat and the collector controller are on, the flow diverters move the circulating fluid between the load and exchanger 2. If the thermostat is off and the collector controller is on, the diverters move the circulating fluid between the storage unit and exchanger 2. Finally, when the thermostat is on and the collector controller is off, the diverters move the circulating fluid between the storage unit and the load.

System II (the standard liquid-based system) differs from all the other systems simulated in this investigation in that the storage unit (a conventional water tank) can be charged and discharged simultaneously. Hence, instead of describing it in terms of its modes of operation, it is more appropriate to describe it as three independently operating subsystems, viz. the collector loop, the load, and the domestic hot water system. Whenever solar energy is available, it is collected and transferred to the storage unit. Whenever a space heating load is present, it is met by the storage unit and the auxiliary energy source. The domestic hot water system draws energy from the storage unit when necessary.

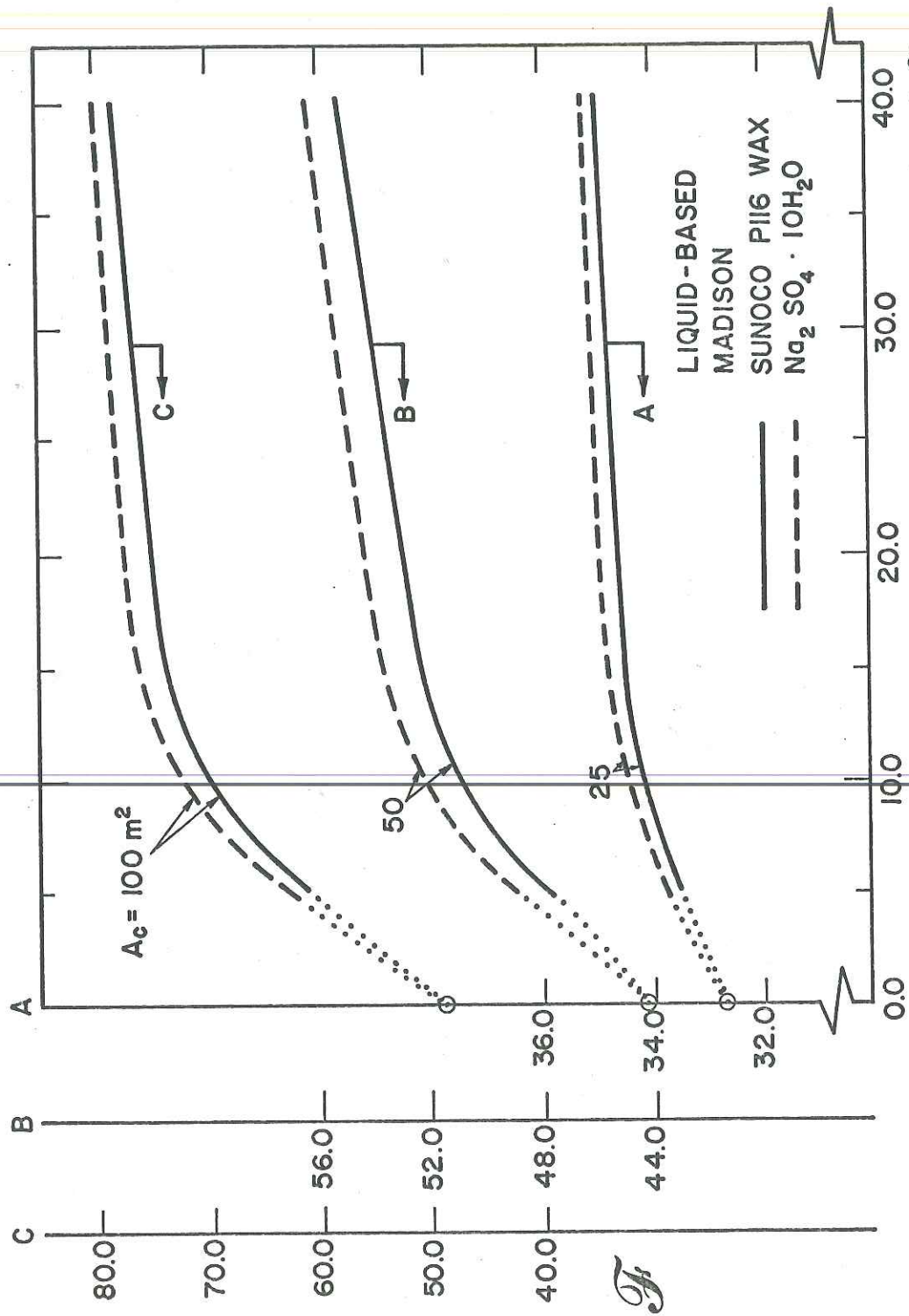
System II is also controlled by a two stage thermostat and two on/off differential controllers. One on/off controller monitors the collector outlet temperature and the storage unit temperature and controls pumps 1 and 2. The other on/off controller monitors the storage unit and pre-heat water tank temperatures and controls pumps 4 and 5. The thermostat monitors the room temperature and controls pump 3 and the auxiliary energy source.

System III has only one mode of operation: whenever a space heating load is present it is met by the available solar energy and the auxiliary energy source when necessary. It is controlled by a two-stage thermostat and one on/off differential controller. The thermostat monitors the room temperature and controls the auxiliary energy source and pumps 1 and 3. The on/off controller compares the collector outlet temperature with the preheat water tank temperature and controls pump 2.

### 3.4 Results for Liquid-Based Systems

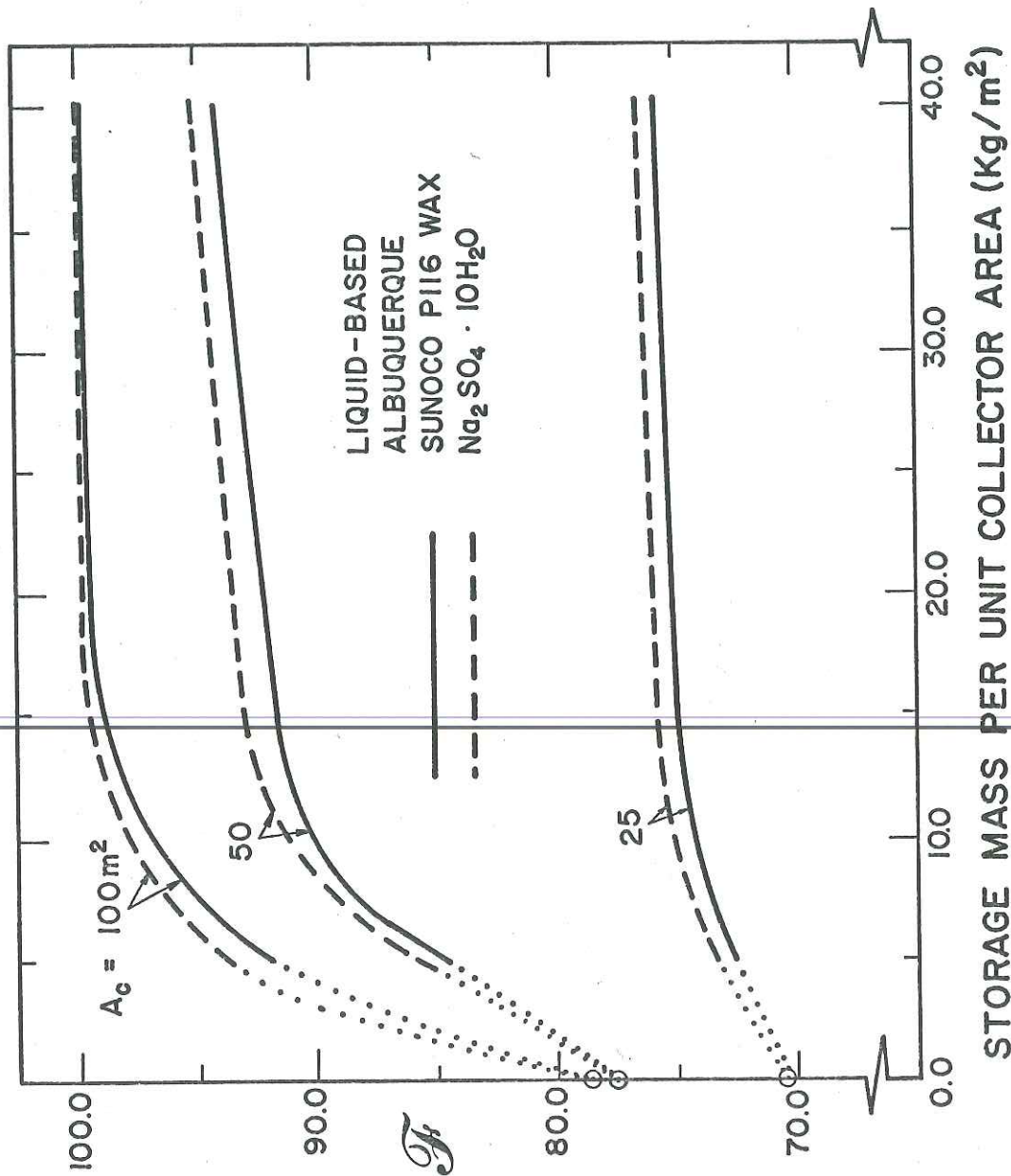
Liquid-based systems utilizing two different PCM's were simulated for two locations. As in the air-based system investigation, sodium sulfate decahydrate and paraffin wax were examined for Madison and Albuquerque.

Figures 21 and 22 show the effect of storage capacity on the long-term performance of liquid-based systems in



**STORAGE MASS PER UNIT COLLECTOR AREA ( $\text{Kg/m}^2$ )**

FIGURE 21. Variation of Solar-Supplied Fraction of Load with Storage Mass and Collector Area for Liquid Based Systems Utilizing PCES in Madison.



**STORAGE MASS PER UNIT COLLECTOR AREA ( $\text{Kg/m}^2$ )**

FIGURE 22. Variation of Solar-Supplied Fraction of Load with Storage Mass and Collector Area for Liquid-Based Systems Utilizing PCES in Albuquerque.

Madison and Albuquerque respectively. These results pertain to the System I configuration except those at zero storage capacity, where System III is used. It is clear that the use of  $\text{Na}_2\text{SO}_4 \cdot 10\text{H}_2\text{O}$  yields slightly better system performance than for those utilizing the same mass of paraffin wax. Similar results were also found for air-based systems and again, it can be attributed to the higher latent heat and lower melting temperature of the  $\text{Na}_2\text{SO}_4 \cdot 10\text{H}_2\text{O}$ .

Figures 21 and 22 can be used to determine an optimum range of storage capacities for liquid-based systems in the same manner as Figures 8 and 9 were used for air-based systems. Figure 21 shows that in Madison, no significant improvement in system performance is realized by increasing the storage mass beyond about  $20 \text{ Kg/m}^2$  for both  $\text{Na}_2\text{SO}_4 \cdot 10\text{H}_2\text{O}$  and paraffin wax. System performance drops off significantly when the storage mass is smaller than approximately  $7 \text{ Kg/m}^2$ . Figure 9 shows this range to be roughly 7 to  $15 \text{ Kg/m}^2$  for both PCM's in Albuquerque.

Therefore, based solely on system thermal performance, the storage mass per unit collector area should be  $7 - 20 \text{ Kg/m}^2$  for systems utilizing these materials. Again, as was stated for air-based systems, the values in the upper end of the range apply to locations characterized by relatively large heating loads and low amounts of incident solar energy (e.g. Madison). As the heating load decreases and the incident solar energy increases (e.g. Albuquerque) the necessary storage size decreases. In either case, economics will dictate the optimum storage size.

The performance results for a system utilizing a conventional water tank are shown in Figure 23. This data pertains to System II; the standard liquid-based system. The storage was modeled as a fully-mixed water tank with no stratification effects.

In Figure 24 the performance results for systems utilizing PCES are compared with those utilizing water tank storage. It is clear that, over the range of practical storage sizes, the sensible heat storage yields higher  $F$  values than the PCES.

In Figure 25, the results of Figure 24 are replotted in terms of storage volume per unit collector area. This figure shows that, for liquid-based systems, PCES does not compare as favorably with sensible heat storage as it did for air-based systems. In fact, a system utilizing paraffin wax will require a larger storage volume than a system with a water tank. For example, a system utilizing 0.036 cubic meters per unit collector area of paraffin wax will realize an  $F$  value of 53.1. This identical system performance can be achieved using either a 0.027 cubic feet per unit collector area water tank or 0.015 cubic feet per unit collector area of  $\text{Na}_2\text{SO}_4 \cdot 10\text{H}_2\text{O}$ .

Therefore, a liquid-based system utilizing  $\text{Na}_2\text{SO}_4 \cdot 10\text{H}_2\text{O}$ , in Madison will require approximately one-half the storage volume of a water tank system in order to achieve the same system performance. On the other hand, a system utilizing

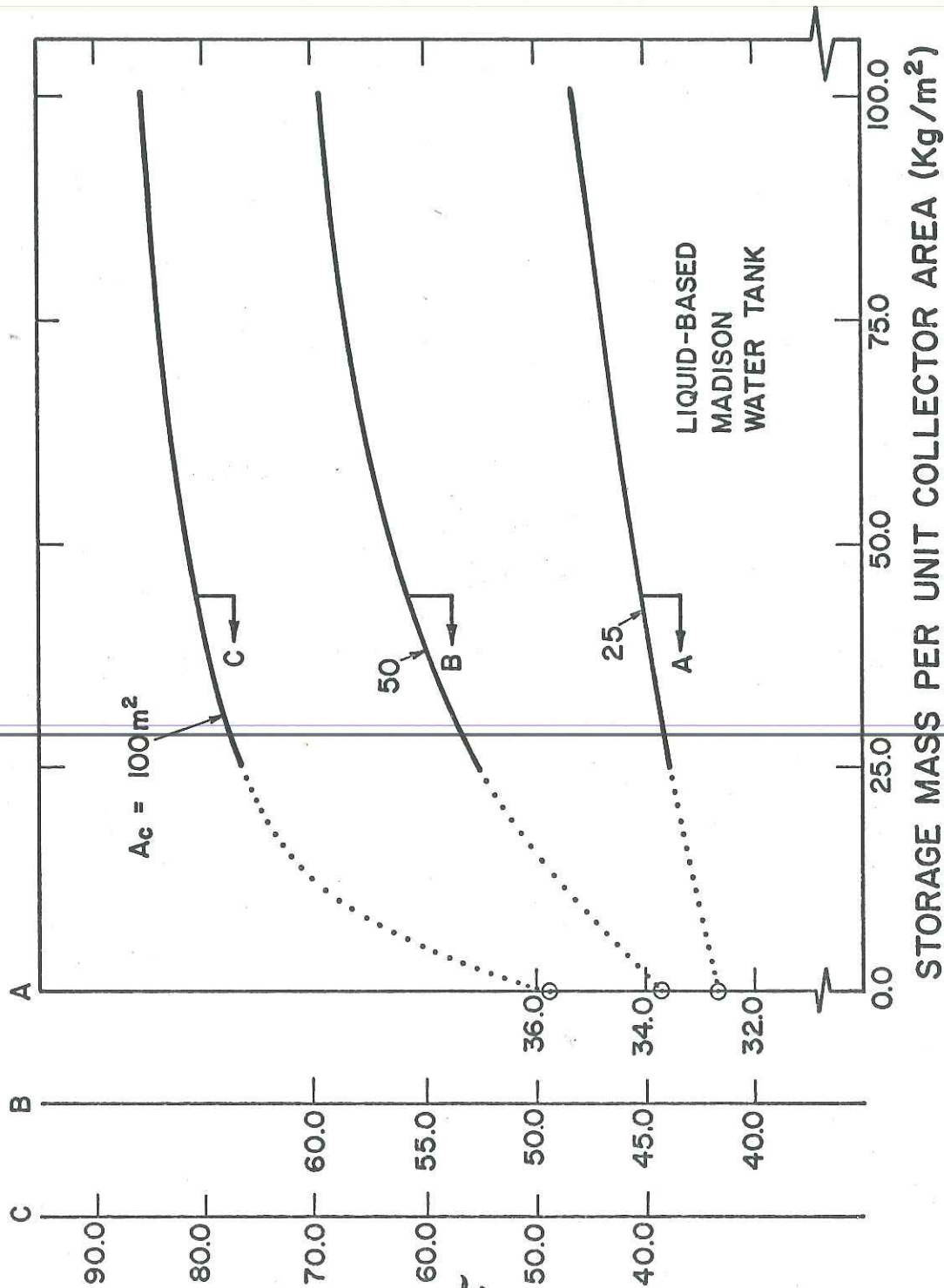


FIGURE 23. Variation of Solar-Supplied Fraction of Load with Storage Mass and Collector Area for Liquid-Based Systems Utilizing Water Tank Storage in Madison.

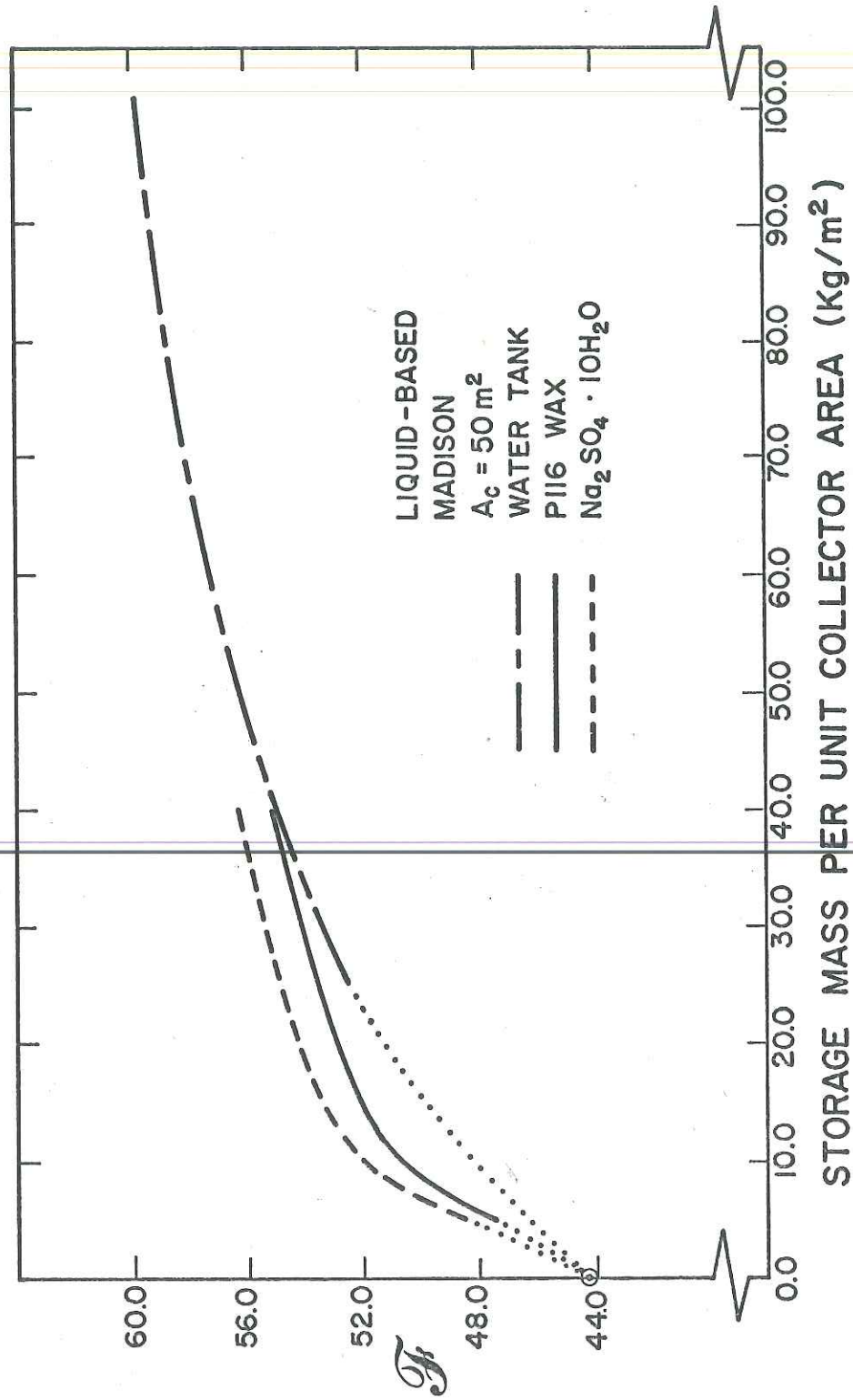


FIGURE 24. Variation of Solar-Supplied Fraction of Load with Storage Mass for Liquid-Based Systems Utilizing Sensible and Latent Heat Storage Media In Madison.

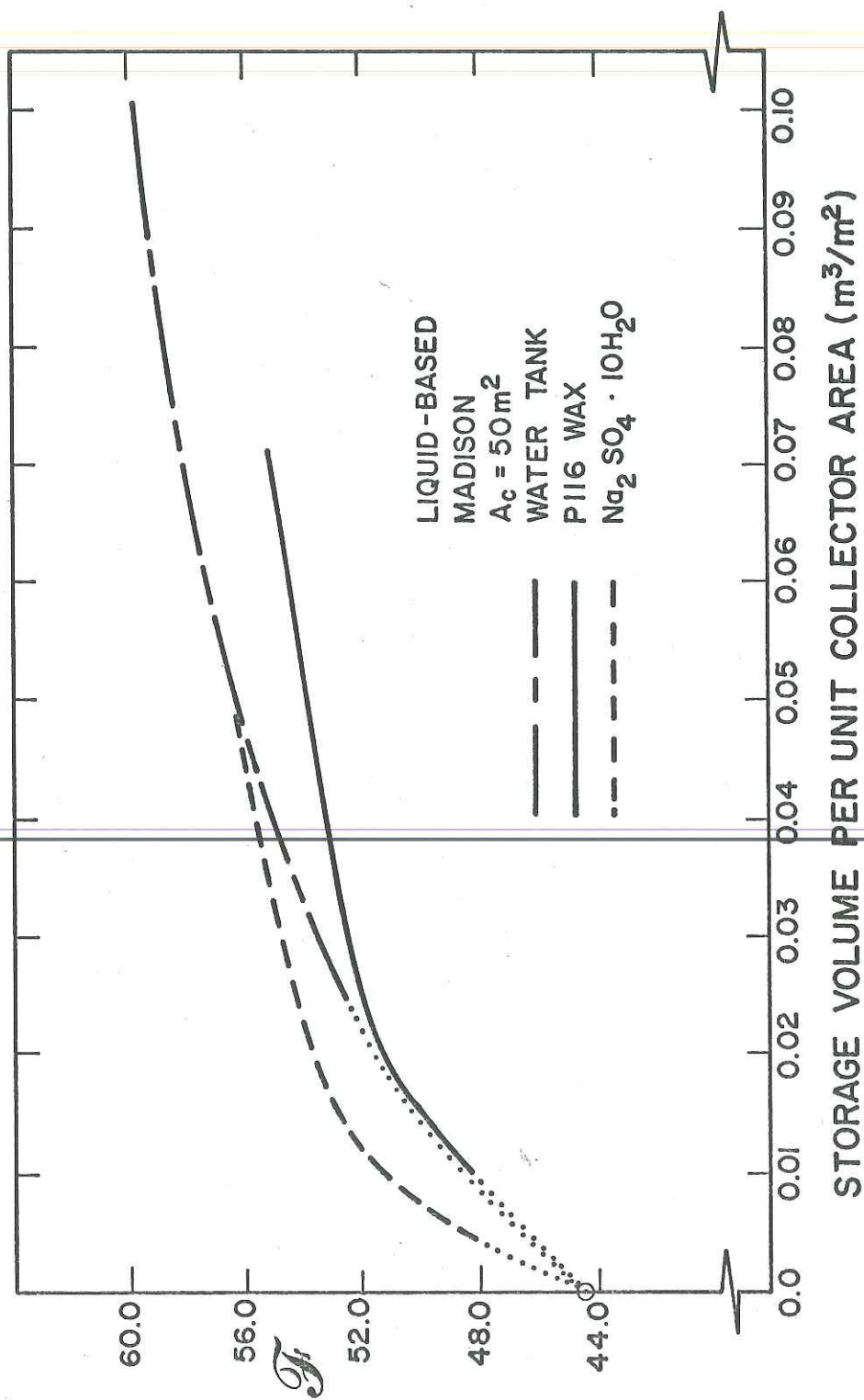
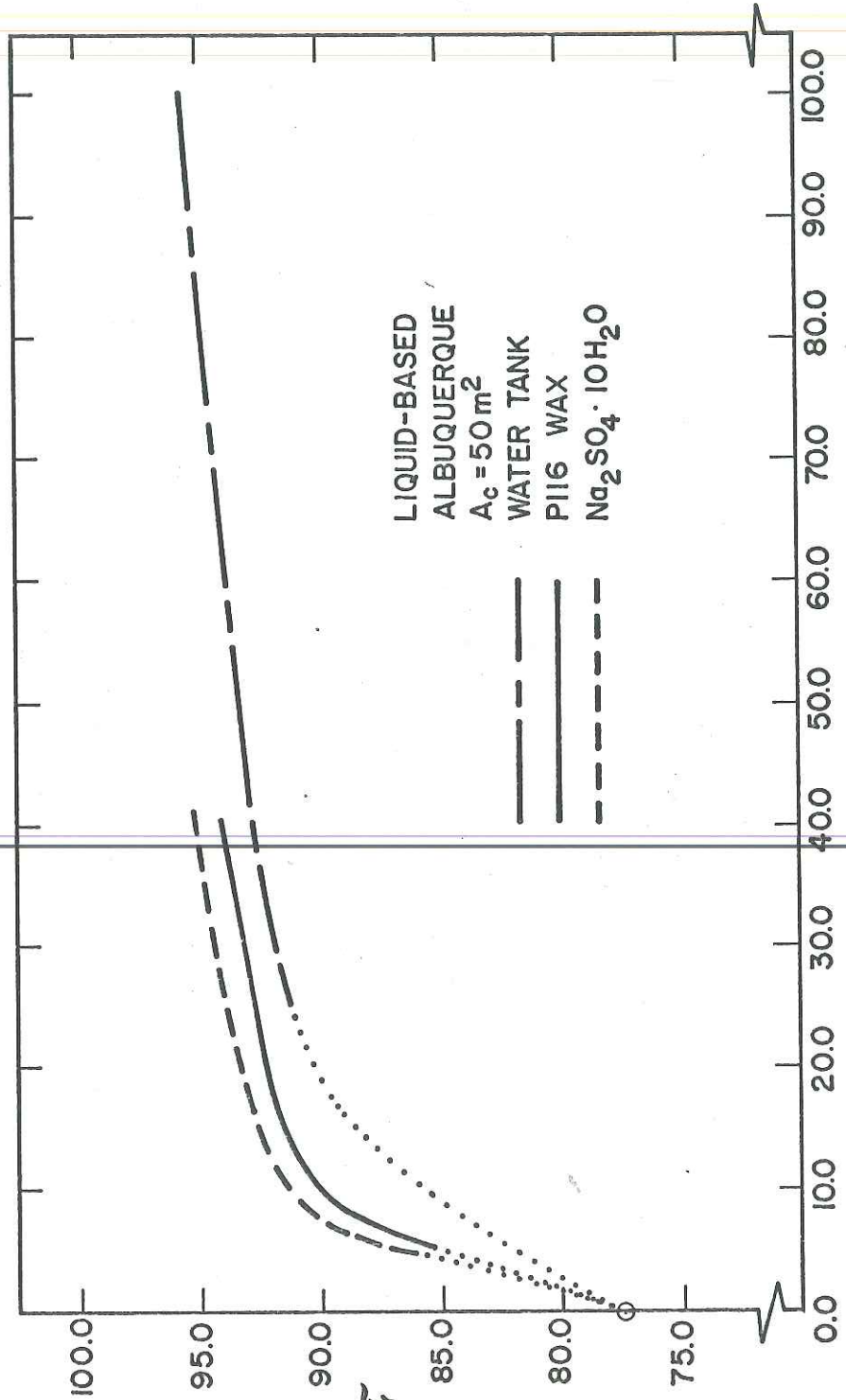


FIGURE 25. Variation of Solar-Supplied Fraction of Load with Storage Volume for Liquid-Based Systems Utilizing Sensible and Latent Heat Storage Media in Madison.

paraffin wax will require 25 percent more storage volume than a system with a water tank to yield the same system performance.

In Figures 26 and 27, the comparison between sensible and latent heat storage is shown for Albuquerque. These results are consistent with those for Madison. For example, a system utilizing a water tank with a volume of 0.027 cubic meters per unit collector area will realize an  $F$  value of 91.5. This identical system performance can be achieved using either the same volume of paraffin wax or 0.014 cubic meters per unit collector area of  $\text{Na}_2\text{SO}_4 \cdot 10\text{H}_2\text{O}$ . Here again, a system utilizing  $\text{Na}_2\text{SO}_4 \cdot 10\text{H}_2\text{O}$  will require approximately one-half the storage volume of a water tank system to realize the same system performance. On the other hand, a system utilizing paraffin wax will require a storage volume equivalent to that of a water tank system to achieve the same system performance.



**STORAGE MASS PER UNIT COLLECTOR AREA ( $\text{Kg}/\text{m}^2$ )**

FIGURE 26. Variation of Solar-Supplied Fraction of Load with Storage Mass for Liquid-Based Systems Utilizing Sensible and Latent Heat Storage Media in Albuquerque.

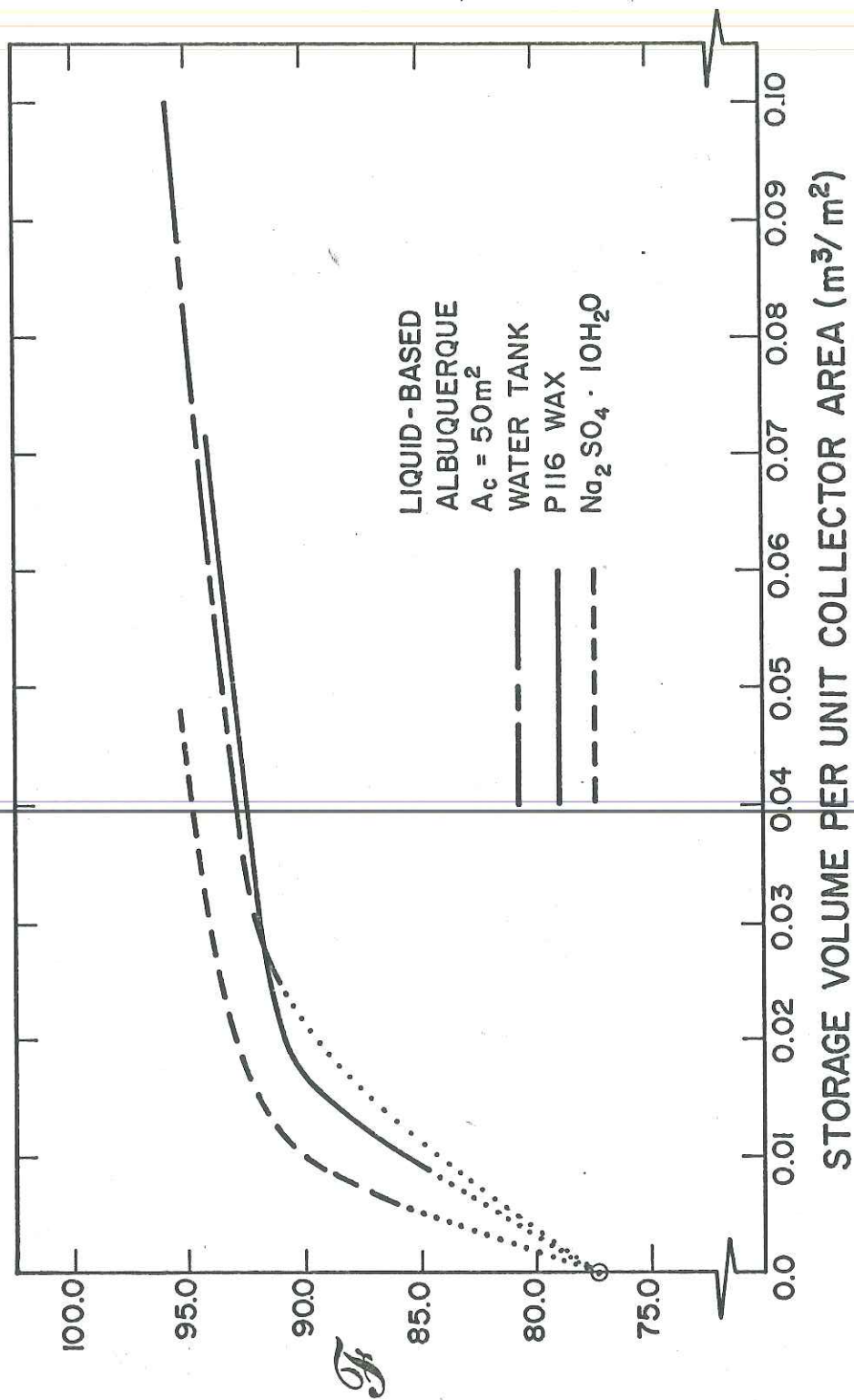


FIGURE 27. Variation of Solar-Supplied Fraction of Load with Storage Volume for Liquid-Based Systems Utilizing Sensible and Latent Heat Storage Media in Albuquerque.

## CHAPTER 4

## DISCUSSION, CONCLUSIONS AND RECOMMENDATIONS

The first objective of this work was to develop a practical model describing the long-term transient behavior of PCES units for incorporation into the simulation program TRNSYS [14]. This resulted in the creation of six PCES models each representing a different level of approximation. They are listed below:

1. A general model capable of simulating PCES in either air-based or liquid-based systems. No restrictions were placed upon the type of circulating fluid since its capacitance was accounted for.
2. A negligible fluid capacitance model for air-based systems.
3. ~~An infinite NTU, negligible fluid capacitance model for air-based systems.~~
4. An infinite NTU, negligible fluid capacitance, and variable properties model for air-based systems.
5. An infinite NTU model for liquid-based systems.
6. An infinite NTU, variable properties model for liquid-based systems.

The second objective of this work was to employ the above models in long-term simulations to determine the effects of storage/exchanger NTU, storage size, material properties and location on system performance. This portion of the investigation lead to the following conclusions:

1. Solar heating system performance is relatively insensitive to the storage/exchanger NTU within the practical design range. The results show that varying the NTU from a value of one to infinity will not result in any significant change in system performance. Consequently, two related conclusions can be drawn. First, with little error and considerably reduced computational costs, an infinite NTU model can be used to describe practical PCES units. Second, considerable freedom can be exercised in the design of PCES units and the containment of PCM's with regard to the resulting storage/exchanger NTU.

2. Based on the thermal performance of the system, optimum storage capacities per unit collector area will be in the range of 7-20 kg/m<sup>2</sup> for the Na<sub>2</sub>SO<sub>4</sub>·10H<sub>2</sub>O and 7-25 kg/m<sup>2</sup> for paraffin wax in both air-based and liquid-based systems. ~~The optimum storage capacity is location dependent with the~~ values in the upper end of the ranges applying to locations characterized by relatively large heating loads and low amounts of incident solar energy (e.g. Madison). As the heating load decreases and the incident solar energy increases (e.g. Albuquerque) the necessary storage size decreases. Ultimately, the optimum storage capacity will depend upon the system economics. As the initial and operating costs of the system decrease and the price of auxiliary fuel increases, the optimum storage capacity will move to the higher values in the given ranges.

3. Systems utilizing Na<sub>2</sub>SO<sub>4</sub>·10H<sub>2</sub>O will perform slightly better than those utilizing the same mass of paraffin wax,

provided that the thermal properties of the salt do not degrade upon repeated thaw/freeze cycling. This is due to the lower melting temperature and larger latent heat of  $\text{Na}_2\text{SO}_4 \cdot 10\text{H}_2\text{O}$  which result in lower collector inlet temperatures and hence, higher collector efficiencies.

The final objective of this work was to compare the performance of systems utilizing PCES with those utilizing conventional rock bed and water tank storage. The following conclusions can be drawn:

1. Over the range of practical storage sizes, systems utilizing sensible heat storage will have slightly higher  $\mathcal{F}$  values than those with PCES. This is true for both liquid-based and air-based systems in any location and independent of the "quality" of the collector (i.e. the overall energy loss coefficient). Obviously, as the storage capacity approaches infinity, the fraction of the load supplied by solar will approach the same value for systems using either sensible or latent heat storage media. This is also the case as the storage capacity approaches zero.

2. For air-based systems, the storage volume required for the utilization of PCES will be considerably smaller than that required for sensible heat storage. PCES in paraffin wax will require one-half the storage volume of a rock bed system and  $\text{Na}_2\text{SO}_4 \cdot 10\text{H}_2\text{O}$  only one-fourth in order to achieve the same system performance.

For liquid-based systems, PCES will not realize the significant savings in storage volume that it can for air-based systems. This is due to the relatively large heat capacity of water ( $4.19 \text{ KJ/KG}^\circ\text{C}$ ), which is more than three times that of rock on a volume basis. A system utilizing paraffin wax will require roughly the same storage volume as a water tank system in order to achieve an identical system performance. A system utilizing  $\text{Na}_2\text{SO}_4 \cdot 10\text{H}_2\text{O}$  will require approximately one-half the storage volume of a water tank system in order to realize the same system performance. These results are also independent of location and collector "quality".

Ultimately, the comparison between sensible and latent heat storage will depend upon their relative costs. In order to gain some insight into storage unit economics, a simple cost comparison can be made between a PCES unit and a rock bed for an air-based heating system. For example, consider a house in Madison with a heating requirement of  $1000 \text{ KJ/hr}^\circ\text{C}$  and 50 square meters of collector. Figure 12 shows that the fraction of the load supplied by solar will be 47.5 using 5.5 cubic meters ( $\sim 200$  cubic feet) of rock. Contractors are currently installing rock beds at a cost of  $\$2\text{-}3/\text{ft}^3$ . This figure is for containers constructed with two inch by six inch studs and plywood for walls, two inch by four inch studs and plywood for the cover, and adequate

insulation. At \$4 to \$6 a ton ( $\sim$  25 cents per cubic foot) the rock itself accounts for only about 10 percent of the total cost. Based on these figures, a rock bed for this system would cost between \$400 and \$600.

Referring again to Figure 12, a PCES unit for this system would require 1.2 cubic meters ( $\sim$ 42 cubic feet) of  $\text{Na}_2\text{SO}_4 \cdot 10\text{H}_2\text{O}$  in order to achieve an  $\mathcal{F}$  value of 47.5. This would include the flow channels and 2200 pounds of the PCM. According to Telkes [8], the material can be packaged in plastic trays at a cost of \$8 per 100 pounds. Commercial producers claim the cost is currently as high as \$25 per 100 pounds. Hence, the packaging costs could range from \$176 to \$550 for this application.

The container in which the PCM trays are placed could be similar in construction to the stud and plywood type used for rock beds. If the cost is assumed to be the same (i.e.  $\$2\text{-}3/\text{ft}^3$  minus the cost of the rock which was included), then the PCES container would cost between \$75 and \$115.

The cost of  $\text{Na}_2\text{SO}_4 \cdot 10\text{H}_2\text{O}$  is currently around \$11 per 1,000 pounds (including the nucleating and thickening ingredients) according to Telkes [8]. Hence, the material costs for this unit would be \$24.

Therefore, the total cost for a PCES unit for this system would be between \$275 and \$690. Surprisingly, this is in the same range as the estimated rock bed cost.

Obviously, the costs used above may not be exact.

However, this simple example has illustrated an important point: the higher costs of PCM's compared to rock may be offset by the dramatic savings associated with a smaller container.

#### 4.1 Recommendations

This thesis began with a discussion which grouped the past work in PCES into two areas: 1) material selection, testing, and containment; and 2) theoretical modeling. Continuation of work in both areas is recommended as follows:

1) The models described in this work assume that the PCM behaves in an idealized way and hence, the results represent an upper bound to system performance. The capability of these PCES models should be expanded to include radial conduction, supercooling, crystallization, environmental losses and possibly, property degradation caused by cycling. These phenomena could significantly affect system performance.

2. A sensitivity study could be performed to optimize the thermal properties of PCM's for solar heating applications. This information would be useful in screening and selecting potential PCM candidates.

3. Use of a histogram in computer simulations would make it possible to determine PCM cycling characteristics (i.e. the frequency and duration of thaw/freeze cycles).

This information would be invaluable when considering PCM's whose thermal properties degrade upon repeated cycling.

4. A complete economic analysis is necessary in order to determine the optimum storage capacities for PCM's and the practicality of PCES compared to conventional storage media.

5. Prior to this investigation, no work had been done to determine the performance of complete solar energy systems utilizing PCES. The computer simulations described in this thesis form the basis for experimental work which must follow. PCES units should be installed in real systems, instrumented, and monitored to determine their cycling characteristics and effect on the performance of real systems. Currently, Solar House I at the University of Delaware is the only working system utilizing PCES which is completely instrumented for this purpose.

## APPENDIX A

Weather Data

This investigation employed weather data for two locations: Madison (WI) and Albuquerque (NM). The data for Albuquerque consisted of hourly solar radiation, ambient temperature, wind speed, and wind direction for the year 1959. The data for Madison consisted of hourly solar radiation, ambient temperature, wind speed and wind direction for an "average" or "typical" year.

The "average" year for Madison was constructed from the years 1948 through 1956. The incident solar radiation and ambient temperature were averaged for every month in the eight year period. Each month of the "average" year was determined by selecting the month during the 8 year period which was closest to the 8 year average for that month.

Klein et al. [16] developed the "average" year for Madison and investigated the possibility of using it with simulation models to estimate long-term system performance. They simulated four solar systems using each of the 8 years of Madison weather data and the "average" year. They found that although there were significant variations in system performance over the 8 year period, the average performance for the 8 years was very close to the performance resulting from the "average" year. They concluded that the "average" year can be used to represent weather data occurring in the long-term.

## APPENDIX B

Computer Listings

Two computer models are listed on the following pages: the infinite NTU, negligible circulating fluid capacitance, variable properties model for air-based systems (Type 28), and the infinite NTU, variable properties model for liquid-based systems (Type 27). These versions were the most extensively used in this investigation.

Explanation of Variables

A	-	PCM cross sectional area
AF	-	circulating fluid channel cross sectional area
CF	-	circulating fluid specific heat
CL	-	specific heat of PCM in liquid phase
CS	-	specific heat of PCM in solid phase
D	-	density of PCM
DF	-	density of circulating fluid
DT	-	subroutine time step
DELU	-	change in internal energy of storage unit from initial value
FLOWT-		mass flow rate from collectors
FLOWB-		mass flow rate from load
FT	-	fraction of run time mass flow is from collectors (storage charging)

FB	-	fraction of run time mass flow is from load (storage discharging)
FO	-	fraction of run time mass flow is off (storage isolated)
IFLOW-		integer representing either charging (1) or discharging (2)
N	-	number of subroutine time steps within each TRNSYS time step
OUT	-	subroutine output array
Q	-	energy transferred to PCM during a time step
QTNK	-	energy supplied to load from the storage unit
TIME	-	current simulation time
TIMETR-		TRNSYS time step
TINT	-	initial temperature of PCM
TM	-	melting temperature of PCM
TREF	-	reference temperature for PCM internal energy
TFT	-	temperature of circulating fluid entering PCES unit
TFB	-	temperature of circulating fluid entering PCES unit from the load
XAV	-	average quality of PCM
XINT	-	initial quality of PCM
XKL	-	thermal conductivity of PCM in liquid phase
XKS	-	thermal conductivity of PCM in solid phase
XL	-	length of PCES unit
XLH	-	PCM latent heat
XIN	-	subroutine input array
U	-	PCM specific internal energy

## TYPE 28

```

C*****
C INFINITE NTU MODEL FOR AIR-BASED SYSTEMS
C AIR CAPACITANCE IS NEGLECTED
C VARIATION OF PROPERTIES BETWEEN THE SOLID AND LIQUID PHASES
C OF THE PHASE CHANGE MATERIAL ARE ACCOUNTED FOR
C*****
SUBROUTINE TYPE28(TIME,XIN,OUT,T,DTDT,PAR,INFO)
DIMENSION XIN(5),OUT(15),PAR(30),INFO(8),U(20),TS(20),X(20)
1 ,TTEM(20),UTEM(20),XTEM(20),USAV(20),
1 TSSAV(20),XSAV(20)
INFO(6) = 14

C
C-----DETERMINE TRNSYS TIME STEP
C
IF(SAVE.GT.0.0) GOTO 101
IF(INFO(7).EQ.-1) SAVE = 0.0
TIMETR = (TIME - SAVE)
SAVE = TIME
IF(INFO(7).EQ.-1) INDEX = 0
INDEX = INDEX + 1
IF(INDEX.EQ.2) GOTO 80
IF(INDEX.EQ.3) GOTO 101

C
C-----EQUATE SUBROUTINE VARIABLES TO TRNSYS DATA
C
XLH=PAR(1)
CS=PAR(2)
CL=PAR(3)
XKS=PAR(4)
XKL=PAR(5)
D=PAR(6)
A=PAR(7)
CF=PAR(8)
TM=PAR(9)
N=PAR(10)
XL=PAR(11)
TINT=PAR(12)
XINT=PAR(13)
SC=PAR(14)

C
101 TREF = 0.
TFT = XIN(1)
FLOWT = XIN(2)
TFB = XIN(3)
FLOWB = XIN(4)

C
C-----DETERMINE FLOW DIRECTION
C
IF(FLOWB.LE..1E-6) GOTO 3
FLOW = FLOWB
TF1 = TFB
IFLOW= 2
GOTO 4

```

```

3 FLOW = FLOWT
  TF1 = TFT
  IFLOW= 1
4 CONTINUE

C
C-----CALCULATE PARAMETER GROUPS
C
  XK1 = (FLOW * CF) / (D * A)
  IF(INFO(7).NE.-1) GOTO 102
  XK2 = XKL / D
  US = CS * (TM - TREF)
  UL = US + XLH
  NM1 = N - 1
  DZ = XL / N
102 DT = TIMETR

C
C-----CALCULATE MULTIPLIERS AND MODES
C
  IF(FLOW.LE..1E-6) GOTO 444
  XMAX = (XK1 * DT) / (DZ * CL)
  MODE = 1
  GOTO 5
444 XMAX = (2. * XK2 * DT) / ((DZ ** 2.) * CL)
  MODE = 2
  5 CONTINUE

C
C-----STABILITY CHECK AND TIME INTERVAL CHANGE
C
  STABLE = SC
  IF(XMAX.LE.STABLE) GOTO 6
  NM = IFIX((XMAX / SC) + 1.)
  DT = DT / NM
  GOTO 66
  6 CONTINUE
  NM = 1
  66 CONTINUE

C
C-----DETERMINE INITIAL VALUES OF U,T,TF,X AND SKIP TO OUTPUTS
C
  IF(INFO(7).NE.-1) GOTO 8
  IF(TINT.GT.TM) GOTO 222
  UINT = CS * (TINT - TREF) + (XINT * XLH)
  GOTO 667
222 UINT = CS * (TM - TREF) + XLH + CL * (TINT - TM)
667 UAV = UINT
  DO 7 I=1,N
  U(I) = UINT
  TS(I) = TINT
  X(I) = XINT
  7 CONTINUE
  PER = 0.0
  FT = 0.0
  FB = 0.0
  FO = 0.0

```

```

      QTNK = 0.0
      GOTO 80
      8 CONTINUE
C
C-----SAVE U,TF,TS,X ON FIRST CALL OF TIME STEP
C
      IF(INFO(7).NE.0) GOTO 778
      DO 777 I=1,N
      USAV(I) = U(I)
      TSSAV(I) = TS(I)
      XSAV(I) = X(I)
777 CONTINUE
      PERSAV = PER
      FTSAV = FRTOP
      FBSAV = FRBOT
      FOSAV = FROFF
      QSAV = QTNK
      GOTO 889
778 DO 888 I=1,N
      U(I) = USAV(I)
      TS(I) = TSSAV(I)
      X(I) = XSAV(I)
888 CONTINUE
      PER = PERSAV
      FRTOP = FTSAV
      FRBOT = FBSAV
      FROFF = FOSAV
      QTNK = QSAV
889 CONTINUE
C
C-----REVERSE INDICES
C
      IF(IFLOW.EQ.1) GOTO 666
      DO 11 I=1,N
      TTEM(I) = TS(I)
      UTEM(I) = U(I)
      11 CONTINUE
      DO 12 I=1,N
      INEW = N + 1 - I
      TS(INEW) = TTEM(I)
      U(INEW) = UTEM(I)
      12 CONTINUE
C
C-----TRNSYS LOOP STARTS HERE
C
      666 Q = 0.0
      DO 500 JJ=1,NM
      IF(MODE.EQ.2) GOTO 27
C
C-----UPDATE INTERNAL ENERGY *** (FLOW MODE) ***
C
      U(1) = U(1) + (XK1 * DT * (TF1 - TS(1)) / DZ)
C
      DO 26 I=2,N

```

```

      IM1 = I - 1
C
      U(I) = U(I) + (XK1 * DT * (TS(IM1) - TS(I)) / DZ)
26 CONTINUE
      GOTO 155
C
C-----UPDATE INTERNAL ENERGY *** CONDUCTION MODE ***
C
27 XK = X(1) * XKL + (1 - X(1)) * XKS
      XKP = X(2) * XKL + (1 - X(2)) * XKS
      U(1) = U(1) + (DT * (XKP * TS(2) - XK * TS(1)) / ((DZ ** 2) * D))
C
      DO 34 I=2,NM1
      IP1 = I + 1
      IM1 = I - 1
      XK = X(I) * XKL + (1 - X(I)) * XKS
      XKP = X(IP1) * XKL + (1 - X(IP1)) * XKS
      XKM = X(IM1) * XKL + (1 - X(IM1)) * XKS
C
      U(I) = U(I) + DT * (XKP * TS(IP1) - 2 * XK * TS(I)
1          + XKM * TS(IM1)) / ((DZ ** 2) * D)
34 CONTINUE
      XK = X(N) * XKL + (1 - X(N)) * XKS
      XKM = X(NM1) * XKL + (1 - X(NM1)) * XKS
C
      U(N) = U(N) + (DT * (XKM * TS(NM1) - XK * TS(N)) / ((DZ ** 2) * D))
C
C-----UPDATE TEMPERATURE AND QUALITY
C
155 DO 38 I=1,N
      IF(U(I).GT.US) GOTO 35
      TS(I) = (U(I) / CS) + TREF
      X(I) = 0.0
      GOTO 37
35 IF(U(I).LT.UL) GOTO 36
      TS(I) = ((U(I) - UL) / CL) + TM
      X(I) = 1.0
      GOTO 37
36 TS(I) = TM
      X(I) = (U(I) - US) / XLH
37 CONTINUE
38 CONTINUE
C
C-----DETERMINE ENERGY TRANSFER TO FLUID IN BOTTOM FLOW MODE
C
      IF(IFLOW.EQ.1) GOTO 499
      QSTEP = FLOW * CF * (TS(N) - TF1) * DT
      Q = Q + QSTEP
499 CONTINUE
500 CONTINUE
C
C-----INTERNAL INTEGRATION OF QTNK
C
      QTNK = QTNK + Q

```

```

C
C-----REVERSE INDICES
C
      IF(IFLOW.EQ.1) GOTO 63
      DO 61 I=1,N
      TTEM(I) = TS(I)
      UTEM(I) = U(I)
      XTEM(I) = X(I)
61 CONTINUE
      DO 62 I=1,N
      INEW = N + 1 - I
      TS(INEW) = TTEM(I)
      U(INEW) = UTEM(I)
      X(INEW) = XTEM(I)
62 CONTINUE
63 CONTINUE

C
C-----DETERMINE AVERAGE INTERNAL ENERGY AND STORE
C
      SUM = 0.0
      DO 64 I=1,N
      SUM = SUM + U(I)
64 CONTINUE
      UAV = (SUM / FLOAT(N))
      DELU = (UAV - UINT) * A * XL * D

C
C-----DETERMINE AVERAGE QUALITY
C
      XSUM = 0.0
      DO 88 I=1,N
      XSUM = XSUM + X(I)
88 CONTINUE
      XAV = XSUM / FLOAT(N)

C
C-----FRACTION RUN TIME IN TWO PHASE
C
      IPER = 0
      IF(XAV.GT.0.) IPER = 1
      PER = PER + TIMETR * FLOAT(IPER)
      IF(TIME.LT..001) GOTO 80
      XPER = PER / TIME

C
C-----FRACTION RUN TIME WITH FLOW ON
C
      ITOP = 0.0
      IBOT = 0.0
      IOFF = 0.0
      IF(FLOWT.GT.0.) ITOP = 1.0
      IF(FLOWB.GT.0.) IBOT = 1.0
      IF(FLOW.LT..1E-6) IOFF = 1.0
      FRTOP = FRTOP + TIMETR * FLOAT(ITOP)
      FRBOT = FRBOT + TIMETR * FLOAT(IBOT)
      FROFF = FROFF + TIMETR * FLOAT(IOFF)

C

```

```
FT = FRTOP / TIME  
FB = FRBOT / TIME  
FO = FROFF / TIME
```

```
80 CONTINUE
```

```
C
```

```
C-----OUTPUT NOMENCLATURE
```

```
C
```

```
OUT(1) = TS(N)  
OUT(2) = FLOWT  
OUT(3) = TS(1)  
OUT(4) = FLOWB  
OUT(5) = DELU  
OUT(6) = QTNK  
OUT(7) = XPER  
OUT(8) = UAV  
OUT(9) = XAV  
OUT(10) = 0.0  
OUT(11) = FLOAT(NM)  
OUT(12) = FT  
OUT(13) = FB  
OUT(14) = FO  
RETURN  
END
```

## TYPE 27

```

C*****
C INFINITE NTU MODEL FOR LIQUID-BASED SYSTEMS
C VARIATION OF PROPERTIES BETWEEN THE SOLID AND LIQUID PHASES
C OF THE PHASE CHANGE MATERIAL IS ACCOUNTED FOR
C*****
      SUBROUTINE TYPE27(TIME,XIN,OUT,T,DTDT,PAR,INFO)
C
C***** INFINITE NTU STORAGE FOR WATER SYSTEMS *****
C
      DIMENSION XIN(5),OUT(15),PAR(30),INFO(8),PSI(20),TS(20),X(20)
      1 ,TTEM(20),PSITEM(20),XTEM(20),PSISAV(20),
      1 TSSAV(20),XSAV(20)
      INFO(6) = 14
C
C-----DETERMINE TRNSYS TIME STEP
C
      IF(SAVE.GT.0.0) GOTO 101
      IF(INFO(7).EQ.-1) SAVE = 0.0
      TIMETR = (TIME - SAVE)
      SAVE = TIME
      IF(INFO(7).EQ.-1) INDEX = 0
      INDEX = INDEX + 1
      IF(INDEX.EQ.2) GOTO 80
      IF(INDEX.EQ.3) GOTO 101
C
C-----EQUATE SUBROUTINE VARIABLES TO TRNSYS DATA
C
      XLH=PAR(1)
      CS=PAR(2)
      CL=PAR(3)
      XKS=PAR(4)
      XKL=PAR(5)
      D=PAR(6)
      A=PAR(7)
      DF=PAR(8)
      AF=PAR(9)
      CF=PAR(10)
      XKF=PAR(11)
      TM=PAR(12)
      XL=PAR(13)
      N=PAR(14)
      TINT=PAR(15)
      XINT=PAR(16)
      SC=PAR(17)
C
      101 TREF = 0.
          TFT = XIN(1)
          FLOWT = XIN(2)
          TFB = XIN(3)
          FLOWB = XIN(4)
C
C-----DETERMINE FLOW DIRECTION
C

```

```

IF(FLOWB.LE..1E-6) GOTO 3
FLOW = FLOWB
TF1 = TFB
IFLOW= 2
GOTO 4
3 FLOW = FLOWT
TF1 = TFT
IFLOW= 1
4 CONTINUE

```

```

C
C-----CALCULATE PARAMETER GROUPS
C

```

```

XK1 = (FLOW * CF) / (D * A)
IF(INFO(7).NE.-1) GOTO 102
XK2 = (DF * AF * CF) / (D * A)
XK3 = (XKF * AF) / (D * A)
PSIS = CS * (TM - TREF) + XK2 * TM
PSIL = PSIS + XLH
NM1 = N - 1
DZ = XL / N
102 DT = TIMETR

```

```

C
C-----CALCULATE MULTIPLIERS AND MODES
C

```

```

IF(FLOW.LE..1E-6) GOTO 444
XMAX = (XK1 * DT) / (DZ * (CL + XK2))
MODE = 1
GOTO 5
444 XMAX = (((XKL / D) + XK3) * DT) / ((DZ ** 2.) * (CL + XK2))
MODE = 2
5 CONTINUE

```

```

C
C-----STABILITY CHECK AND TIME INTERVAL CHANGE
C

```

```

STABLE = SC
IF(XMAX.LE.STABLE) GOTO 6
NM = IFIX((XMAX / SC) + 1.)
DT = DT / NM
GOTO 66
6 CONTINUE
NM = 1
66 CONTINUE

```

```

C
C-----DETERMINE INITIAL VALUES OF PSI,T,X AND SKIP TO OUTPUTS
C

```

```

IF(INFO(7).NE.-1) GOTO 8
IF(TINT.GE.TM) GOTO 222
PSINT = CS * (TINT - TREF) + XK2 * TINT
GOTO 667
222 PSINT = CS * (TM - TREF) + (XK2 * TINT) + (XINT * XLH)
1 + CL * (TINT - TM)
667 PSIAV = PSINT
DO 7 I=1,N
PSI(I) = PSINT

```

```

      TS(I) = TINT
      X(I) = XINT
7 CONTINUE
      PER = 0.0
      FT = 0.0
      FB = 0.0
      FO = 0.0
      QTNK = 0.0
      GOTO 80
8 CONTINUE
C
C-----SAVE PSI,TS,X ON FIRST CALL OF TIME STEP
C
      IF(INFO(7).NE.0) GOTO 778
      DO 777 I=1,N
      PSISAV(I) = PSI(I)
      TSSAV(I) = TS(I)
      XSAV(I) = X(I)
777 CONTINUE
      PERSAV = PER
      FTSAV = FRTOP
      FBSAV = FRBOT
      FOSAV = FROFF
      QSAV = QTNK
      GOTO 889
778 DO 888 I=1,N
      PSI(I) = PSISAV(I)
      TS(I) = TSSAV(I)
      X(I) = XSAV(I)
888 CONTINUE
      PER = PERSAV
      FRTOP = FTSAV
      FRBOT = FBSAV
      FROFF = FOSAV
      QTNK = QSAV
889 CONTINUE
C
C-----REVERSE INDICES
C
      IF(IFLOW.EQ.1) GOTO 666
      DO 11 I=1,N
      TTEM(I) = TS(I)
      PSITEM(I) = PSI(I)
11 CONTINUE
      DO 12 I=1,N
      INEW = N + 1 - I
      TS(INEW) = TTEM(I)
      PSI(INEW) = PSITEM(I)
12 CONTINUE
C
C-----TRNSYS LOUP STARTS HERE
C
666 Q = 0.0
      DO 500 JJ=1,NM

```

```

IF(MODE.EQ.2) GOTO 27
C
C-----UPDATE INTERNAL ENERGY *** (FLOW MODE) ***
C
PSI(1) = PSI(1) + (XK1 * DT * (TF1 - TS(1)) / DZ)
C
DO 26 I=2,N
IM1 = I - 1
C
PSI(I) = PSI(I) + (XK1 * DT * (TS(IM1) - TS(I)) / DZ)
26 CONTINUE
GOTO 155
C
C-----UPDATE INTERNAL ENERGY ***(CONDUCTION MODE)***
C
27 F1 = ((X(1) * XKL + (1 - X(1)) * XKS) / D) + XK3
F2 = ((X(2) * XKL + (1 - X(2)) * XKS) / D) + XK3
PSI(1) = PSI(1) + (F2 * TS(2) - F1 * TS(1)) * DT / (DZ ** 2)
C
DO 34 I=2,NM1
IP1 = I + 1
IM1 = I - 1
FM = ((X(IM1) * XKL + (1 - X(IM1)) * XKS) / D) + XK3
F = ((X(I) * XKL + (1 - X(I)) * XKS) / D) + XK3
FP = ((X(IP1) * XKL + (1 - X(IP1)) * XKS) / D) + XK3
C
PSI(I) = PSI(I) + (FP * TS(IP1) - 2. * F * TS(I) + FM * TS(IM1))
1 * DT / (DZ ** 2)
34 CONTINUE
FNM = ((X(NM1) * XKL + (1 - X(NM1)) * XKS) / D) + XK3
F = ((X(N) * XKL + (1 - X(N)) * XKS) / D) + XK3
C
PSI(N) = PSI(N) + (FNM * TS(NM1) - F * TS(N)) * DT / (DZ ** 2)
C
C-----UPDATE TEMPERATURE AND QUALITY
C
155 DO 38 I=1,N
IF(PESI(I).GE.PSIS) GOTO 35
TS(I) = (PSI(I) + (CS * TREF)) / (CS + XK2)
X(I) = 0.0
GOTO 37
35 IF(PESI(I).LE.PSIL) GOTO 36
TS(I) = (PSI(I) - XLH - CS * (TM - TREF) + CL * TM) / (XK2 + CL)
X(I) = 1.0
GOTO 37
36 TS(I) = TM
X(I) = (PSI(I) - CS * (TM - TREF) - XK2 * TM) / XLH
37 CONTINUE
38 CONTINUE
C
C-----DETERMINE ENERGY TRANSFER TO FLUID IN BOTTOM FLOW MODE
C
IF(IFLOW.EQ.1) GOTO 499
QSTEP = FLOW * CF * (TS(N) - TF1) * DT

```

```

      Q      = Q + QSTEP
499 CONTINUE
500 CONTINUE
C
C-----INTERNAL INTEGRATION OF QTNK
C
      QTNK = QTNK + Q
C
C-----REVERSE INDICES
C
      IF(IFLOW.EQ.1) GOTO 63
      DO 61 I=1,N
      TTEM(I) = TS(I)
      PSITEM(I) = PSI(I)
      XTEM(I) = X(I)
61 CONTINUE
      DO 62 I=1,N
      INEW = N + 1 - I
      TS(INEW) = TTEM(I)
      PSI(INEW) = PSITEM(I)
      X(INEW) = XTEM(I)
62 CONTINUE
63 CONTINUE
C
C-----DETERMINE AVERAGE INTERNAL ENERGY AND STORE
C
      SUM = 0.0
      DO 64 I=1,N
      SUM = SUM + PSI(I)
64 CONTINUE
      PSIAV = (SUM / FLOAT(N))
      DELU = (PSIAV - PSINT) * A * XL * D
C
C-----DETERMINE AVERAGE QUALITY
C
      XSUM = 0.0
      DO 88 I=1,N
      XSUM = XSUM + X(I)
88 CONTINUE
      XAV = XSUM / FLOAT(N)
C
C-----FRACTION RUN TIME IN TWO PHASE
C
      IPER = 0
      IF(XAV.GT.0.) IPER = 1
      PER = PER + TIMEIR * FLOAT(IPER)
      IF(TIME.LT..001) GOTO 80
      XPER = PER / TIME
C
C-----FRACTION RUN TIME WITH FLOW ON
C
      ITOP = 0.0
      IBOT = 0.0
      IOFF = 0.0

```

```
IF(FLOWT.GT.0.) ITOP = 1.0
IF(FLOWB.GT.0.) IBOT = 1.0
IF(FLOW.LT..1E-6) IOFF = 1.0
FRTOP = FRTOP + TIMETR * FLOAT(ITOP)
FRBOT = FRBOT + TIMETR * FLOAT(IBOT)
FROFF = FROFF + TIMETR * FLOAT(IOFF)
```

C

```
FT = FRTOP / TIME
FB = FRBOT / TIME
FO = FROFF / TIME
```

80 CONTINUE

C

C-----OUTPUT NOMENCLATURE

C

```
OUT(1) = TS(N)
OUT(2) = FLOWT
OUT(3) = TS(1)
OUT(4) = FLOWB
OUT(5) = DELU
OUT(6) = QTNK
OUT(7) = XPER
OUT(8) = PSIAV
OUT(9) = XAV
OUT(10) = O.U
OUT(11) = FLOAT(NM)
OUT(12) = FT
OUT(13) = FB
OUT(14) = FO
RETURN
END
```

## APPENDIX C

Considerations When Using Finite DifferenceApproximations With an Infinite NTU Model

This appendix will discuss the difficulties involved in using a finite differencing scheme with an infinite NTU model.

Consider an "infinite" - NTU storage unit with a uniform initial temperature  $T_1$ . The circulating fluid enters the unit at a rate of  $\dot{m}$  and a temperature  $T_2$  greater than  $T_1$ . Because of the infinite NTU, over a time interval  $\Delta t$ , a portion of the storage material  $M$  (represented by the cross hatched area in Figure C.1.) will be raised to the temperature  $T_2$ . As time proceeds the temperature front propagates through the unit until all the phase change material reaches  $T_2$ .

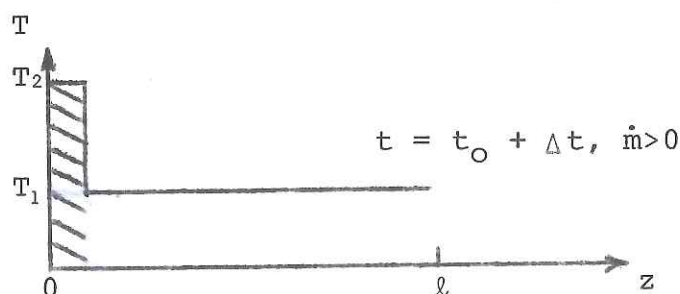


Figure C.1.

The portion of the storage material  $M$  which has its specific internal energy raised from  $u_1$  to  $u_2$  can be determined from a simple energy balance as follows:

$$\dot{m}c_f(T_2 - T_1)\Delta t = M(u_2 - u_1) \quad (C.1.)$$

Here,  $\dot{m}c_f(T_2 - T_1)\Delta t$  represents the energy transferred from the circulating fluid to the storage material during the time interval  $\Delta t$ . Rearranging equation C.1. to solve for  $M$  yields:

$$M = \frac{\dot{m}c_f(T_2 - T_1)\Delta t}{(u_2 - u_1)} \quad (\text{C.2.})$$

$M$  can also be represented by the following relationship:

$$M = \rho A v \Delta t \quad (\text{C.3.})$$

Here,  $v$  is the velocity at which the temperature front propagates through the storage unit.

Substituting equation C.3. into C.2. will yield the following relationship for  $v$ :

$$v = \frac{\dot{m}c_f(T_2 - T_1)}{\rho A (u_2 - u_1)} \quad (\text{C.4.})$$

The problem which arises when using a spatial finite difference approximation for an infinite NTU model is that it introduces a smearing or smoothening of the square wave temperature front. For example, consider a storage unit with an initial temperature distribution and nodal spacing as shown in Figure C.2.

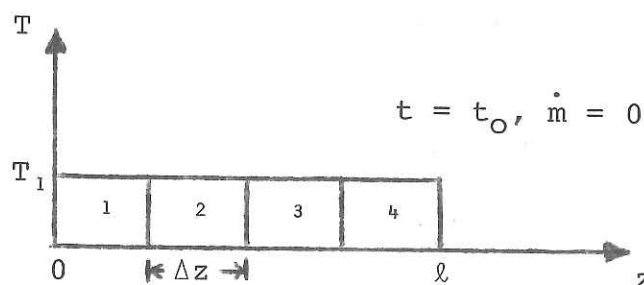


Figure C.2.

During a time interval  $\Delta t$ , the circulating fluid enters the unit at a rate  $\dot{m}$  and temperature  $T_2$ . If it is assumed that a portion of the storage material  $M$  is raised to a temperature  $T_2$ , then the wave front should resemble the hatched area in Figure C.3. However, if  $M$  is not an integer multiple of the nodal mass, then the temperature front resulting from a finite difference approximation will be averaged over the entire node as illustrated by the dotted curve in Figure C.3.

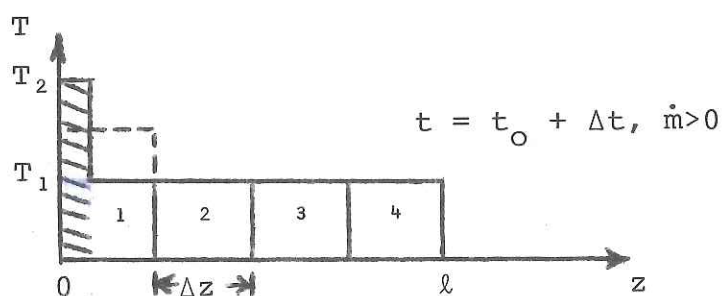


Figure C.3.

Obviously, the accuracy of the finite difference approximation will depend upon the number of nodes. As the number of nodes increases, the smearing effect becomes less pronounced. Hughes et al. [14] encountered this effect in their infinite NTU model for rock beds. They came to the conclusion that five nodes represented a reasonable compromise between computing costs and accuracy.

During this investigation, the number of nodes in the infinite NTU PCES model was varied from eleven to five. It was found that the performance results of the storage

subsystem varied by only one half of one percent. Therefore, all of the simulations performed in this investigation employed five nodes.

## BIBLIOGRAPHY

1. Erwin, Guy, "Solar Heating Storage Based on Chemical Reactions," Proceedings of the Workshop on Solar Energy Storage Subsystems for Heating and Cooling of Buildings, pp. 91-95, Charlottesville, Virginia (1975).
2. Altman, Manfred, et. al., "Conservation and Better Utilization of Electric Power by Means of Thermal Energy Storage and Solar Heating--Final Summary Report," NSF/RANN/SE/GI27976/PR73/5, University of Pennsylvania, July 31, 1973.
3. Lane, G. A., Glen, D. N., Clarke, E. C., Rossow, H. E., Quigley, S. W., Drake, S. S., Best, J. S., "Heat-of-Fusion Systems for Solar Energy Storage", Proceedings of Workshop on Solar Energy Storage Subsystems for Heating and Cooling of Buildings, pp. 43-55, Charlottesville, Virginia (1975).
4. Hale, D. V., Hoover, M. J., and O'Neill, M. J., "Phase Change Materials Handbook", NASA CR-61363.
5. Denton, Jesse C., "Phase Change Storage Systems Group Report", Proceedings of the Workshop on Solar Energy Storage Subsystems for Heating and Cooling of Buildings, p. 169, Charlottesville, Virginia (1975).
6. Lorsch, H. G., "Latent Heat and Sensible Heat Storage for Solar Heating Systems", NSF/RANN/SE/GI27976/TR72/20, University of Pennsylvania, December 1972.
7. Chahroudi, Day, "Suspension Media for Heat Storage Materials", Proceedings of the Workshop on Solar Energy Storage Subsystems for Heating and Cooling of Buildings, p. 56-59, Charlottesville, Virginia, (1975).
8. Telkes, Maria, "Thermal Storage for Solar Heating and Cooling", Proceedings of the Workshop on Solar Energy Storage Subsystems for Heating and Cooling of Buildings, p. 17-23, Charlottesville, Virginia (1975).
9. Bannister, T. C., "Space Thermal Control Using Phase Change", NASA TM X-53402, March 1966.

10. Schlasinger, A. P., and Bentilla, E. W., "Research and Development Study of Thermal Control by Use of Fusible Materials", Northrop Space Laboratories, NSL 65-16, February 1965.
11. Abbott, Stuart, "Computer Program for Prediction of Temperature Profile of Phase Change Observation Test Cell", NASA Working Paper S&E-SSL-TR-WP-6-69, October 1969.
12. Fixler, Sol Z., "Analytical and Experimental Investigation of Satellite Passive Thermal Control Using Phase Change Materials (PCM)", Republic Aviation Corp., Farmingdale, N.Y.
13. Leatherman, R. A., "Component Thermal Control via Heat of Fusion Radiator", ASME-63-AHGT-12, 1963.
14. Hughes, P. J., Klein, S. A., Close, D. J., "Packed Bed Thermal Storage Models for Solar Air Heating and Cooling Systems", Submitted for publication in the ASME Journal of Heat Transfer, (1975).
15. Solar Energy Laboratory UW-Madison, "TRNSYS-A Transient Simulation Program", Engineering Experiment Station Report No. 38, (November 1975).
16. Klein, S. A., Beckman, W. A., Duffie, J. A., "A Design Procedure for Solar Heating Systems", Solar Energy, V. 18, pp. 113-127, (1976).